



Editor's Pick | Virology | Full-Length Text

Neu5Gc binding loss of subtype H7 influenza A virus facilitates adaptation to gallinaceous poultry following transmission from waterbirds

Minhui Guan, ^{1,2,3} Thomas J. DeLiberto, ⁴ Aijing Feng, ^{1,2,3} Jieze Zhang, ⁵ Tao Li, ⁶ Shuaishuai Wang, ⁷ Lei Li, ⁷ Mary Lea Killian, ⁸ Beatriz Praena, ^{1,2,3} Emily Giri, ^{1,2,3} Shelagh T. Deliberto, ⁴ Jun Hang, ⁶ Alicia Olivier, ⁹ Mia Kim Torchetti, ⁸ Yizhi Jane Tao, ¹⁰ Colin Parrish, ¹¹ Xiu-Feng Wan^{1,2,3,12}

AUTHOR AFFILIATIONS See affiliation list on p. 22.

ABSTRACT Between 2013 and 2018, the novel A/Anhui/1/2013 (AH/13)-lineage H7N9 virus caused at least five waves of outbreaks in humans, totaling 1,567 confirmed human cases in China. Surveillance data indicated a disproportionate distribution of poultry infected with this AH/13-lineage virus, and laboratory experiments demonstrated that this virus can efficiently spread among chickens but not among Pekin ducks. The underlying mechanism of this selective transmission remains unclear. In this study, we demonstrated the absence of Neu5Gc expression in chickens across all respiratory and gastrointestinal tissues. However, Neu5Gc expression varied among different duck species and even within the tissues of the same species. The AH/13-lineage viruses exclusively bind to acetylneuraminic acid (Neu5Ac), in contrast to wild waterbird H7 viruses that bind both Neu5Ac and N-glycolylneuraminic acid (Neu5Gc). The level of Neu5Gc expression influences H7 virus replication and facilitates adaptive mutations in these viruses. In summary, our findings highlight the critical role of Neu5Gc in affecting the host range and interspecies transmission dynamics of H7 viruses among avian species.

IMPORTANCE Migratory waterfowl, gulls, and shorebirds are natural reservoirs for influenza A viruses (IAVs) that can occasionally spill over to domestic poultry, and ultimately humans. This study showed wild-type H7 IAVs from waterbirds initially bind to glycan receptors terminated with N-acetylneuraminic acid (Neu5Ac) or N-glycolylneuraminic acid (Neu5Gc). However, after enzootic transmission in chickens, the viruses exclusively bind to Neu5Ac. The absence of Neu5Gc expression in gallinaceous poultry, particularly chickens, exerts selective pressure, shaping IAV populations, and promoting the acquisition of adaptive amino acid substitutions in the hemagglutinin protein. This results in the loss of Neu5Gc binding and an increase in virus transmissibility in gallinaceous poultry, particularly chickens. Consequently, the transmission capability of these poultry-adapted H7 IAVs in wild water birds decreases. Timely intervention, such as stamping out, may help reduce virus adaptation to domestic chicken populations and lower the risk of enzootic outbreaks, including those caused by IAVs exhibiting high pathogenicity.

KEYWORDS H7N9, H7, influenza A virus, transmission, acetylneuraminic acid, N-glycolylneuraminic acid, virus-host interactions, receptor binding, spread, duck

A t least 105 wild bird species from 26 different families have been found to harbor influenza A viruses (IAVs), with waterfowl, gulls, and shorebirds being considered the primary natural reservoirs, particularly *Anseriformes* (ducks, geese, and swans) **Editor** Kanta Subbarao, Université Laval, Laval, Quebec, Canada

Address correspondence to Xiu-Feng Wan, wanx@missouri.edu, or Thomas J. DeLiberto, thomas.i.deliberto@usda.gov.

The authors declare no conflict of interest.

See the funding table on p. 22.

Received 18 January 2024 Accepted 10 July 2024 Published 3 September 2024

Copyright © 2024 American Society for Microbiology. All Rights Reserved.

and *Charadriiformes* (gulls, terns, and waders) (1). This wide range of wild waterbirds maintains a large genetic pool of IAVs, with a total of 16 HA and 9 NA antigenic subtypes. Sporadic spillovers of avian-origin IAVs into domestic poultry are not uncommon, especially in areas with potentially inadequate biosecurity measures. Similar spillovers have also been reported in mammals (i.e., pigs, horses, and dogs) where onward transmission occurred among these new hosts (e.g., avian-like H1N1 in pigs, avian-origin H7N7 in horses, avian-origin H3N8 in horses and dogs, avian-like H3N2 in dogs). There is also potential for these viruses to spill over to humans and other non-reservoir hosts, which creates public and veterinary health burdens.

IAVs typically replicate poorly in a new host following spillover and require adaptation to overcome barriers for efficient replication and transmission. Various host factors have been associated with host adaptation of IAVs, limiting virus reservoir host range. For example, the tissue distribution of the $\alpha 2\text{-}6$ linkage of sialic acids restricts the HA receptor binding ability of avian IAVs, thus limiting their ability to infect humans. In addition, host factors such as $\alpha\text{-importins}$, DDX17 and ANP32A, or ANP32B are involved in polymerase activities that differ among IAVs isolated from avian and mammalian species (2). However, most reports have focused on virus adaptation from avian to mammalian species, or between mammalian species, and the molecular mechanisms of interspecies adaptation among avian species are still not fully understood.

Among all HA subtypes of IAVs, H7 is commonly isolated from wild aquatic birds including dabbling ducks, diving ducks, geese, swans, and shorebirds (1). After being introduced into domestic poultry, H7 viruses can establish and lead to recurrent outbreaks where infected poultry are not depopulated promptly. The recent epizootic in China, caused by A/Anhui/1/2013-lineage H7N9 viruses (AH/13-lineage), led to at least five waves of outbreaks in humans between 2013 and 2018, resulting in 1,567 confirmed human cases, of which 615 were fatal (3), with an increase in cases from late 2016 to early 2017 (4). Notably, this virus was primarily detected in chickens, with less frequent detections in domestic duck species or other gallinaceous poultry such as quail (5–8). A laboratory experiment confirmed that the AH/13-lineage H7N9 virus can efficiently spread through direct contact among chickens but not among Pekin ducks (7). These reports suggest that AH/13-lineage H7N9 viruses have undergone adaptation and acquired effective transmission ability in certain poultry species, particularly chickens, after being introduced from wild birds.

In this study, we investigated the molecular mechanisms underlying avian species barriers in H7 transmission, particularly the factors responsible for the disproportionate distribution of chickens infected with AH/13-lineage H7N9 viruses. We hypothesized that the differential expression of N-glycolylneuraminic acid (Neu5Gc) among avian species exerts selective pressure on H7 IAVs, shaping their evolution and enabling them to replicate and transmit efficiently among gallinaceous poultry, particularly chickens. We compared the glycan binding profiles of H7 IAVs, evaluated the impact of Neu5Gc expression on virus replication and evolution, and identified adaptive mutations affecting receptor binding specificity and replication ability.

RESULTS

The AH/13-lineage H7N9 virus affected chickens more than other domestic avian species

To investigate the distribution of H7 IAVs in avian populations, we downloaded all available H7 sequences (n = 2,651) from public databases (http://www.fludb.org). We sorted them by continent and functional species categories as follows: (i) gallinaceous poultry such as chicken, turkey, quail, guinea fowl, and fowl; (ii) waterfowl such as ducks, geese, and swans, and (iii) all other avian species such as ostrich, ibis, parrot, and unspecified species (Table S1).

Phylogenetic analyses showed that the overall H7 viruses were grouped into Eurasian and North American lineages (Fig. S1a and b). The viruses causing epizootics in domestic poultry, such as H7N1 in Italy (1999–2000) (9), H7N7 in the Netherlands (2003) (10),

H7N3 in Mexico (2012–2013) (11), and AH/13-lineage H7N9 in China (2013–2017) (3), formed unique sub-lineages that were scattered across the phylogenetic tree. In contrast, viruses that caused sporadic spillovers into domestic poultry but were promptly stamped out were represented by individual branch tips mixed with clades of viral sequences recovered from various wild bird species. The majority of data across different species categories originated from Asia and North America (Fig. S1c).

Of the 687 AH/13-lineage H7N9 viruses from poultry across the period when all five waves of outbreaks were detected in humans, 613 (89.23%) were found in chickens, while only 61 (8.88%) were reported from ducks with the majority not specifying the duck species. This is consistent with surveillance data showing that over 90% of AH/13-lineage-positive samples were from chickens (12, 13). In contrast, for non-AH/13-lineage H7 viruses detected in China (n=495), only 182 (36.77%) were found in chickens, compared to 256 (51.72%) detected in ducks, encompassing both wild dabbling ducks and those of unspecified species (Fig. S1d). Of note, due to limited surveillance of avian influenza viruses in wild birds in Eurasia, particularly China, the majority of duck samples analyzed in this study were from domestic poultry.

Taken together, the majority of AH/13-lineage H7N9 viruses were detected in gallinaceous poultry, particularly chickens, whereas the other H7 viruses were generally detected in a wide range of avian species, including a variety of waterfowl and aquatic species, as well as some gallinaceous poultry.

The AH/13-lineage H7N9 virus binds exclusively to Neu5Ac, whereas other H7 viruses from wild dabbling ducks bind to both Neu5Ac and Neu5Gc

To assess receptor binding diversity, we performed glycan microarray experiments on eight AH/13-lineage H7N9 virus strains (i.e., rgSH13, rgCk/WX13, rgCk/DG13, rgCk/WZQ15, rgCk/WZH15, rgCk/HN17, rgDk/GD14, and rgDk/WZ15) and five strains originating from wild waterbirds (i.e., Dk/WV08, rgMall/NL12, Mall/NJ10, rgMall/NJ10, and MuS/RI08) (Table 1). The AH/13-lineage viruses chosen for this study represent a selection from viruses in poultry, which were responsible for the five waves of outbreaks in humans. All 13 H7 viruses tested bound to α 2,3-linked (SA2-3Gal) and α 2,6-linked sialic acids (SA2-6Gal) but not to non-sialic acid glycans (Fig. 1a and b). All viruses showed high affinity for SA2-3Gal but exhibited variations in their binding to SA2-6Gal. All eight AH/13-lineage viruses demonstrated stronger binding signals for SA2-6Gal than the other five viruses from wild waterbirds. We further identified distinct binding patterns among these H7 viruses based on the terminal sialic acid sequence N-acetylneuraminic acid (Neu5Ac) or N-glycolylneuraminic acid (Neu5Gc). Specifically, all eight AH/13-lineage viruses bound exclusively to glycans terminated with Neu5Ac, but not to those terminated with Neu5Gc. In contrast, all five wild waterbird viruses tested showed strong binding preference to glycans terminated with either Neu5Ac or Neu5Gc.

We performed biolayer interferometry analyses for an AH/13-lineage virus, A/chicken/ Wuxi/0405005/2013 (H7N9) (Ck/WX13), and a wild waterbird virus, A/mute swan/Rhode Island/A00325125/2008 (H7N3) (MuS/RI08), to further investigate the results from the glycan microarray analyses. Three testing glycan analogs, Neu5Acα2-3Galβ1-4GlcNAc (3'SLN), Neu5Acα2-3Galβ1-4(Fucα1-3)GlcNAc (sLe^X), and Neu5Acα2-6Galβ1-4GlcNAc (6'SLN), were terminated with Neu5Ac, whereas Neu5Gcα2-3Galβ1-4GlcNAc (3'GLN) and Neu5Gcα2-3Galβ1-4(Fucα1-3)GlcNAc (GLe^X) were terminated with Neu5Gc. To minimize the potential impact of the neuraminidase (NA) and other gene segments, we created two reassortant viruses, rgMuS/RI08 and rgCk/WX13, each containing the HA from the corresponding parent virus aforementioned and all other segments from A/Puerto Rico/8/1934(H1N1) (PR8). Results showed that AH/13-lineage rgCk/WX13 bound exclusively to the three glycan analogs terminated with Neu5Ac but not to the others with Neu5Gc, whereas rgMuS/RI08 bound to all five analogs tested. AH/13-lineage rgCk/WX13 exhibited stronger binding avidity to 6'SLN than rgMuS/RI08. These results support the findings observed in the glycan microarray experiments (Fig. 1c).

TABLE 1 Subtype H7 IAVs and their corresponding abbreviations used in this study

Virus	Accession no. for HA	Abbreviation
Eurasian AH/13-lineage H7N9 from the domestic poultry outbreak in China (2013–2017) ^a		,
A/Shanghai/02/2013(H7N9) (HA,NA) × PR8 ^b (H7N9) ^c	KF021597	rgSH13
A/chicken/Wuxi/0405005/2013(H7N9) (HA) × PR8 (H7N1)	KT779570	rgCk/WX13
A/chicken/Dongguan/3418/2013(H7N9) (HA) × PR8 (H7N1)	KP413395	rgCk/DG13
A/chicken/Wenzhou/RAQL01/2015(H7N9) (HA) × PR8 (H7N1)	KU143278	rgCk/WZQ15
A/chicken/Wenzhou/HATSLG01/2015(H7N9) (HA) × PR8 (H7N1)	KU143283	rgCk/WZH15
A/chicken/Heinan/ZZ01/2017(H7N9) (HA) $^d \times$ PR8 (H7N1)	MF319554	rgCk/HN17
A/Duck/Guangdong/DG527/2014(H7N9)(HA) × PR8 (H7N1)	EPI580283	rgDk/GD14
A/duck/Wenzhou/YJYF24/2015(H7N9) (HA) × PR8 (H7N1)	ALR82230	rgDk/WZ15
Eurasian non-AH/13-lineage H7Nx from waterbirds		
A/mallard/Netherlands/12/2000(H7N7) (HA) × PR8-IBCDC-1 (H7N1) ^c	AY338460	rgMall/NL12
North American non-AH/13-lineage H7Nx from waterbirds		
A/domestic duck/West Virginia/A00140913/2008 (H7N3)	KU289983	Dk/WV08
A/mallard/New Jersey/A00926089/2010 (H7N3)	KU290087	Mall/NJ10
A/mallard/New Jersey/A00926089/2010 (H7N3) (HA) × PR8 (H7N1)	d/New Jersey/A00926089/2010 (H7N3) (HA) × PR8 (H7N1) KU290087	
A/mute swan/Rhode Island/A00325125/2008 (H7N3)	nute swan/Rhode Island/A00325125/2008 (H7N3) KU290204	
A/mute swan/Rhode Island/A00325125/2008 (H7N3) (HA) × PR8 (H7N1)	KU290204	rgMuS/RI08
North American non-AH/13-lineage H7 viruses from domestic poultry (2016–2020)		
A/turkey/Indiana/16-001573-2/2016(H7N8)		Tk/IN1573-16
A/duck/Alabama/17-008643-2/2017(H7N9)		Dk/AL8643-17
A/chicken/Texas/18-007912-2/2018(H7N1)	QKX64971	Ck/TX7912-18
A/turkey/Missouri/18-008108-11/2018(H7N1)	QKX64983	Tk/MO8108-18
A/chicken/Missouri/18-008648/2018(H7N1)		Ck/MO8648-18
A/turkey/California/18-031151-4/2018(H7N3)	AYG99315	Tk/CA1151-18
A/duck/Pennsylvania/19-007197/2019(H7N3)		Dk/PA7197-18
A/guinea fowl/Connecticut/19-009111/2019(H7N3)		Gf/CT9111-19
A/duck/California/19-019071/2019(H7N3)		Dk/CA9071-19
A/turkey/North Carolina/20-007949/2020(H7N3)		Tk/NC7949-20
A/turkey/North Carolina/20-008257/2020(H7N3)		Tk/NC8257-20
A/turkey/North Carolina/20-008425/2020(H7N3)		Tk/NC8425-20
Eurasian AH/13-lineage H7 mutants		
A/chicken/Wuxi/0405005/2013(H7N9) (HA-A122N) × PR8 (H7N1)		A122N ^e
A/chicken/Wuxi/0405005/2013(H7N9) (HA-A135E) × PR8 (H7N1)		A135E
A/chicken/Wuxi/0405005/2013(H7N9) (HA-V179I) × PR8 (H7N1)		V179I
A/chicken/Wuxi/0405005/2013(H7N9) (HA-K193R) × PR8 (H7N1)		K193R

^eAmong these H7 sequences, WX13 was detected in poultry and SH13 in humans during the first wave of outbreaks, DG13 in the second wave, GD14 in the third wave, WZQ15, WZH15, and WZ15 in the fourth wave, and HN17 in the fifth wave.

Taken together, Eurasian AH/13-lineage H7 viruses displayed a different glycan binding profile than those Eurasian and North American H7 from wild waterbirds. Specifically, Eurasian AH/13-lineage viruses were found to bind to only the glycans terminated with Neu5Ac, whereas the wild waterfowl-origin H7 virus in both Eurasia and North America had avidity for both Neu5Ac and Neu5Gc.

Amino acid substitution V179I expands AH/13-lineage H7 virus binding specificity from only Neu5Ac to both Neu5Ac and Neu5Gc

To identify amino acid substitutions responsible for different Neu5Gc binding patterns, we compared the HA sequences of equine H7N7, wild waterbird H7, and AH/13-lineage H7N9 viruses. Equine H7N7 was predicted to bind exclusively to Neu5Gc (14), wild waterbird H7 viruses to both Neu5Ac and Neu5Gc, and AH/13-lineage H7N9 viruses

^bPR8, A/Puerto Rico/8/1934(H1N1).

These viruses were acquired from the BEI resources.

 $[^]d$ The PEVPKRKRTAR/GLFGA cleavage sites were mutated to PEIPKGR/GLFGA to remove multiple basic cleavage sites.

The position was based on H3 numbering. These viruses used in this study are shown in the phylogenetic tree (Fig. S1b).

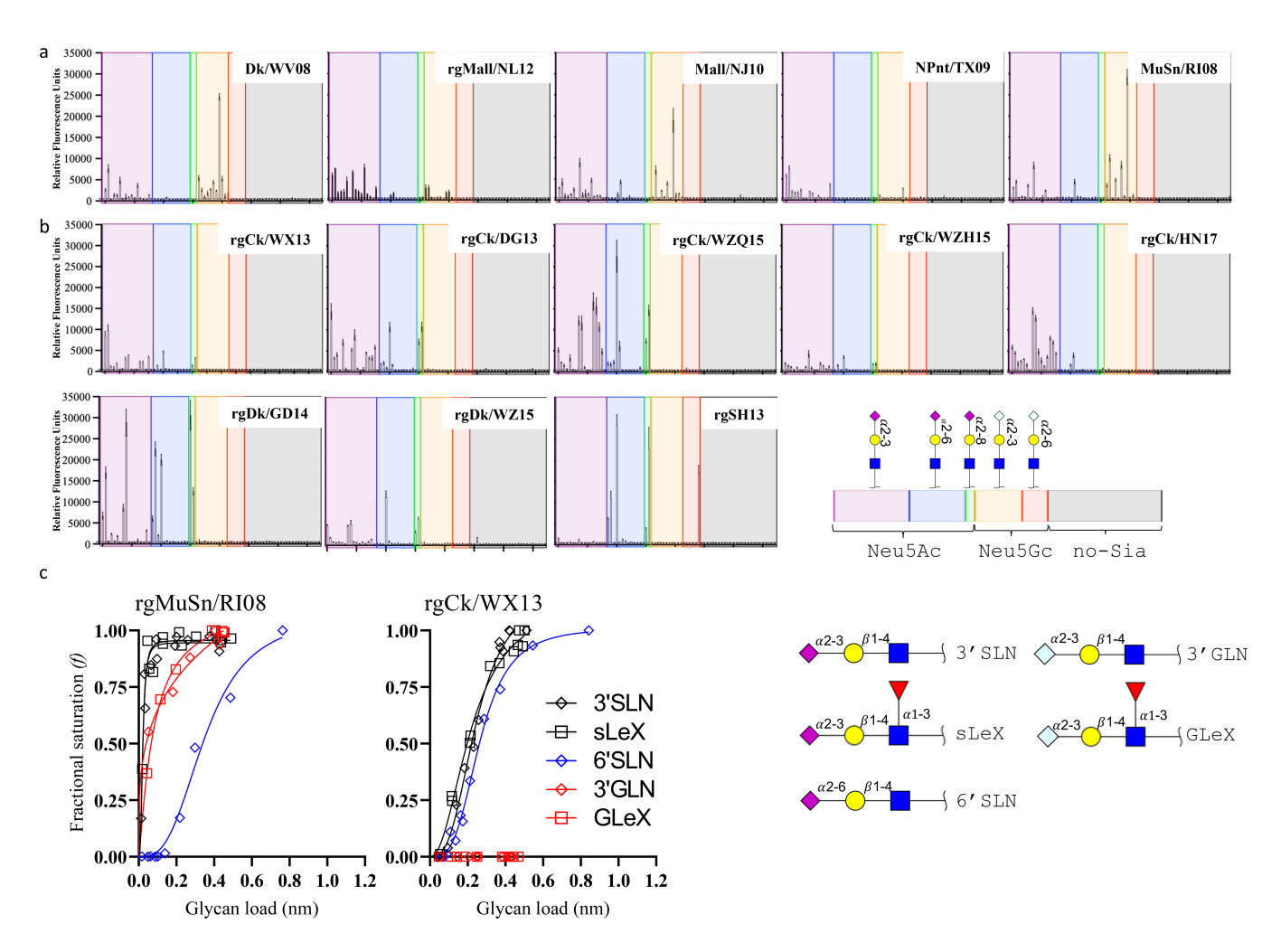


FIG 1 Receptor binding profile of H7 influenza A viruses. (a) N-glycan microarray binding profiles of five H7 viruses isolated from wild waterbirds in Eurasia and North America. (b) N-glycan microarray binding profiles of eight AH/13-lineage H7N9 viruses were collected during the first five waves of outbreaks in humans from 2013 to 2017 in China. (c) Quantitative analyses of virus glycan binding avidity using biolayer interferometry for two representative H7 viruses, rgCk/WX13 and rgMuSn/Rl08 (Table 1). We categorized 75 glycans on the microarray based on the linkage and terminal glycan sequence into α 2,3-linked Neu5Ac, α 2,8-linked Neu5Ac, α 2,8-linked Neu5Gc, and non-sialic acid glycans. The glycan sequences are detailed in Table S5. In the plot showing microarray data, the mean relative fluorescent units \pm the standard deviations (vertical bars) are shown on the y-axis, and the x-axis represents the glycan number corresponding to the array. A microarray contains six replicates of each glycan. Biolayer interferometry analyses were performed using an Octet RED instrument (Pall FortéBio, Fremont, CA, USA) (see Materials and Methods), and binding curves were fitted using the saturation binding method in GraphPad Prism 8 (https://www.graphpad.com/scientific-software/prism/). We quantified and compared the 50% relative sugar loading concentration (RSL_{0.5}) at half the fractional saturation (f = 0.5) of the virus against glycan analogs to determine the binding avidity. A higher RSL_{0.5} indicates a lower binding avidity. The BLI was performed with at least eight concentrations of glycan loadings. In the structures of biotinylated glycan analogs used in BLI, Neu5Aca2-3Galβ1-4GlcNAcβ (3'SLN), Neu5Aca2-6Galβ1-4GlcNAcβ) (6'SLN), Neu5Aca2-3Galβ1-4(Fuca1-3)GlcNAcβ (sLeX), Neu5Gca2-3Galβ1-4GlcNAcβ, Qi'GLN), and Neu5Gca2-3Galβ1-4(Fuca1-3)GlcNAcβ (GLeX), the following glycan symbols were used: light blue diamond indicated Neu5Gc, purple diamond indicated Neu5Ac, yellow circle represents glactose, blue square repre

exclusively to Neu5Ac (Fig. 2). Differences were observed between equine H7N7 viruses and AH/13-lineage H7N9, including three amino acid substitutions [i.e., V130I (H3 numbering), E135A, and R193K; changes from equine H7N7 viruses to AH/13-lineage H7N9] in the receptor binding site (RBS) and seven adjacent to the RBS (i.e., N122A, T128S, V160S, K172R, R173K, E174S, and I179V; changes from equine H7N7 viruses to AH/13-lineage H7N9) (Fig. 2a). Among these 10 positions, only I179 was conserved in both wild waterbird H7 and equine H7, whereas V179 was conserved in AH/13-lineage H7N9, with substitutions identified at the other nine positions.

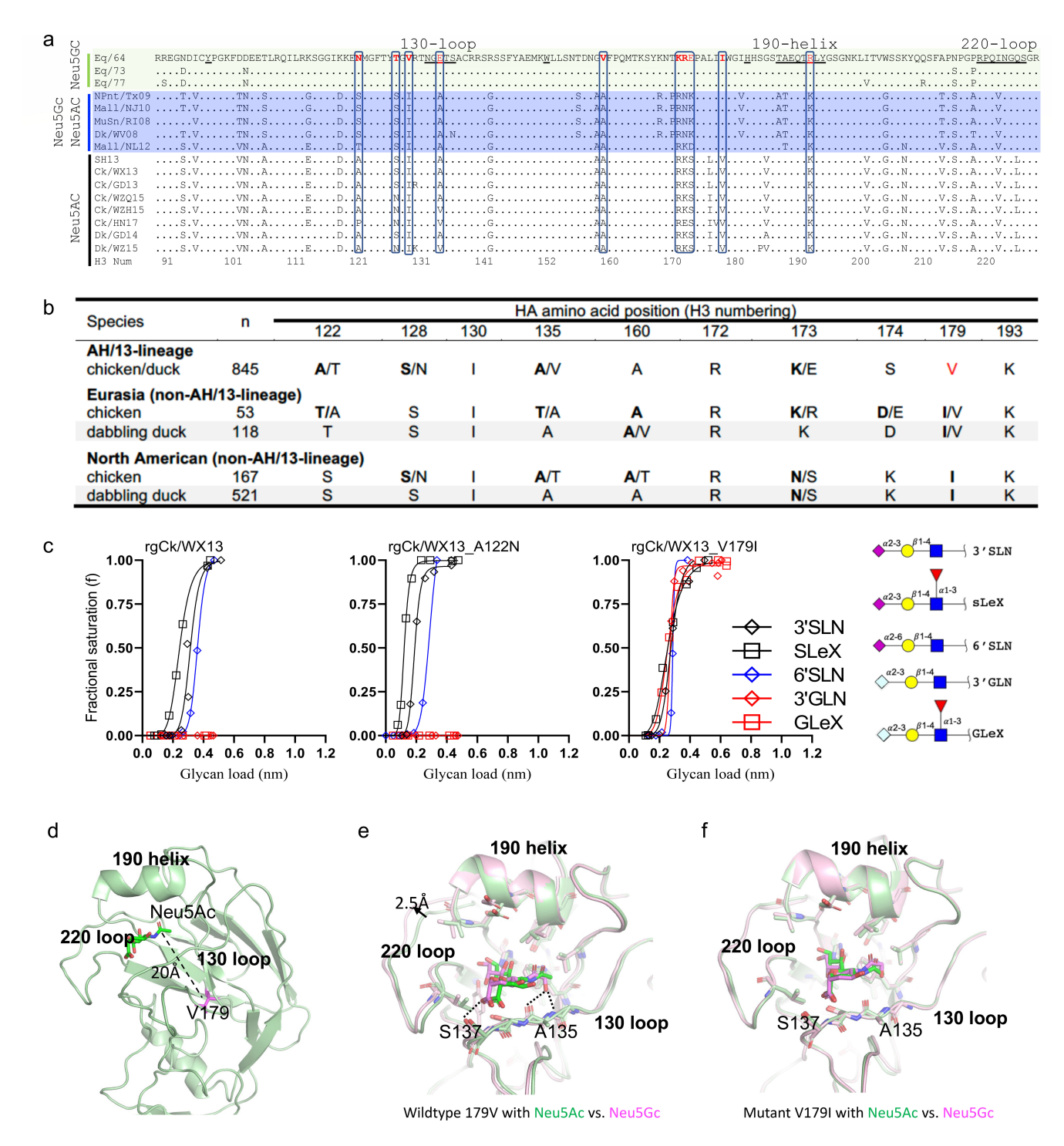


FIG 2 Multiple individual amino acid substitutions facilitate the acquisition of virus binding avidity to Neu5Gc for H7 IAVs. (a) Sequence alignment of the RBS of H7 IAVs, including three groups of H7 viruses with distinct binding patterns to glycans terminated with Neu5Ac and Neu5Gc: equine H7N7 viruses bound exclusively to Neu5Gc, wild waterbird viruses bound to both Neu5Ac and Neu5Gc, and AH/13-lineage H7N9 viruses bound exclusively to Neu5Ac. (b) Amino acid diversity at the residues close to or within the hemagglutinin RBS of AH/13-lineage H7N9 viruses isolated from domestic poultry in China, as well as H7 viruses from dabbling ducks in Eurasia and North America (see additional details in Table 2). (c) Quantitative analyses of virus glycan binding avidity using biolayer interferometry for Ck/WX13, Ck/WX13-A121N, and Ck/WX13-V179I. Please refer to the legend of Fig. 1 and Online Methods for the details of biolayer interferometry analyses. The BLI was performed with at least 8 concentrations of glycan loadings. (d) The crystal structure of the HA protein from A/Anhui/1/2013 (H7N9), is identical to that of Ck/WX13. (e) Structural model of wild-type H7 in complex with Neu5Ac (green) versus Neu5Gc (magenta). HA residues less than 3 Å away from the modeled receptor are shown in sticks. (f) Structural model of the V179I H7 mutant in complex with Neu5Ac (green) versus Neu5Gc (magenta).

We further compared the HA sequences between AH/13-lineage H7N9 viruses and their precursor Eurasian H7 viruses isolated from wild dabbling ducks (15), specifically at the residues mentioned earlier. Amino acid substitutions were detected in the majority of AH/13-lineage isolates at residue 122 and 179 (Fig. 2b). It is noteworthy that amino acid polymorphisms were observed in all ten residues of AH/13-lineage H7N9 viruses, although to a lesser extent in wild waterbirds from both Eurasia and North America (Table S2). Of note, a similar I179V substitution was also observed between poultry-adapted H7N7 viruses in the Netherlands (2003) (with V179) and their precursor virus in wild waterbirds (with I179).

Based on the sequence analyses described above, we designed experiments to further determine the specific residue responsible for the loss of Neu5Gc binding ability in AH/13-lineage viruses. We made the assumption that the necessary amino acids associated with Neu5Gc binding would be conserved between equine and dabbling duck H7 proteins to maintain these bindings. Therefore, we selected the amino acid positions based on two criteria: (i) conservation between dabbling ducks and equines, both of which can bind Neu5Gc, and (ii) complete or partial substitutions between dabbling ducks and chickens, both of which can bind to Neu5Ac. From the analyses (Fig. 2b), only position 179 was selected as our testing target. Additionally, the HA amino acid substitutions A135E and K193R, known to enhance the binding of the H7 virus to Neu5Gc, were included as position controls in this study (16). Residue 122 was also included due to the significant amino acid polymorphisms (including N122) observed at this HA position in AH/13-lineage viruses.

Specifically, we replaced HA V179 (found in AH/13-lineage viruses) with l179 (present in waterfowl/equine H7-like viruses) and then created a reassortant virus rgCk/WX13-V179l. We generated three additional mutants: rgCk/WX13-A122N, rgCk/WX13-A135E, and rgCk/WX13-K193R, by substituting HA positions A122, A135, and K193 in Ck/WX13 with N122, E135, and R139, respectively. Biolayer interferometry analysis revealed that the V179l substitution conferred binding avidity of the AH/13-lineage Ck/WX13 virus to Neu5Gc while maintaining binding to Neu5Ac (Fig. 2c; Fig. S2). A135E and K193R substitutions, as previously reported, enhanced the binding of AH/13-lineage Ck/WX13 virus to Neu5Gc (16), whereas A122N substitution did not significantly affect the virus' glycan binding preference to Neu5Gc or Neu5Ac (Fig. 2c; Fig. S2).

We further performed structural modeling to understand how the amino acid substitution HA I179V enables virus binding from both Neu5Ac and Neu5Gc to Neu5Ac alone. Close inspection of the HA structure shows that V179 (found in poultry-adapted AH/13-lineage viruses) is located at the hydrophobic core of the molecule approximately 20 Å away from the RBS (Fig. 2d). Because this residue is tightly packed against several hydrophobic residues, we hypothesize that V179I, which replaces a poultry-adapted residue with residues characteristic of wild birds, would lead to conformational changes that can propagate to the 130-loop and other structural elements around the RBS and consequently broaden HA binding ability from Neu5Ac to both Neu5Ac and Neu5Gc.

Our modeling results indicate that in the AH/13-lineage H7 (with HA-V179), Neu5Gc occupies a somewhat different position compared to Neu5Ac. Neu5Gc is shifted more toward the 220-loop in the RBS (Fig. 2e). Several close contacts (<3 Å) are observed between Neu5Gc and the RBS, including two between the extra hydroxyl group in Neu5Gc with A135 and one between the carboxyl group at the C2 position with S137 (Fig. 2e). Also, the 220-loop in the Neu5Gc structure is pushed outward by ~2.5 Å, which is presumably necessary to accommodate Neu5Gc in the RBS. These close contacts and the large structural rearrangement of the RBS needed to accommodate Neu5Gc suggest unfavorable binding. Interestingly, the modeled structures of the HA-I179, which are found in waterfowl/equine H7-like viruses, showed very similar binding modes for both Neu5Gc and Neu5Ac (Fig. 2f). In the HA-I179, there is no close contact with Neu5Gc, and the 220-loop in the Neu5Gc complex assumes a nearly identical conformation as in the Neu5Ac complex. This observation explained how the HA-I179 allows the binding to both Neu5Gc and Neu5Ac without any significant structural rearrangement.

Taken together, these results suggest that amino acid substitution V179I, which replaces a poultry-adapted residue with residues characteristic of wild birds, may facilitate the acquisition of binding avidity of AH/13-lineage H7N9 IAVs to Neu5Gc while still maintaining binding to Neu5Ac.

Neu5Gc expression affects H7 virus replication and facilitates the acquisition of adaptive mutations in the HA of H7 IAVs

We hypothesized that the expression of Neu5Gc hinders replication in H7 viruses that exclusively bind to Neu5Ac but do not affect those that bind to both Neu5Ac and Neu5Gc. To test this, we compared the growth kinetics of two mutants (rgCk/WX13-V179I and rgCk/WX13-A122N) and their parent virus, rgCk/WX13, on MDCK-Gc, which overexpress Neu5Gc but still express Neu5Ac (17), and MDCK-wt, the wild-type cell line. Limited Neu5Gc (<1%) was detected in MDCK-wt whereas approximately 40% of their total Sia in MDCK-Gc s Neu5Gc (17). We also included A/mallard/New Jersey/A00926089/2010 (H7N3) (HA)×PR8 (H7N1) (rgMall/NJ10), with the HA of an H7 virus from a mallard (*Anas platyrhynchos*), and A/chicken/Heinan/ZZ01/2017(H7N9) (HA) ×PR8 (H7N1) (rgCk/HN17), with the HA of another AH/13-lineage H7N9 virus from chicken (Table 1). All six viruses tested had identical gene segments except for the HA to minimize the impact of NA and other gene segments (see details in Materials and Methods). Notably, rgCk/WX13-V179I and rgMall/NJ10 bound to both Neu5Ac and Neu5Gc, whereas rgCk/HN17, rgCk/WX13, and rgCk/WX13-A122N bound exclusively to Neu5Ac (Fig. 1 and 2c).

Results indicated that both rgCk/HN17 and rgCk/WX13 viruses showed more efficient replication in MDCK-wt cells than in MDCK-Gc cells (P = 0.0062 and 0.0235, respectively) (Fig. 3a). As expected, rgCk/WX13-A122N displayed similar growth kinetics as its parent virus rgCk/WX13. In contrast, the mutant rgCk/WX13-V179I showed no significant difference in growth kinetics in either cell line, similar to rgMall/NJ10, but different from their respective wild-type parent virus, rgCk/WX13.

To investigate whether Neu5Gc expression shapes the evolution of H7 IAVs, we passaged the rgCk/WX13 and rgMall/NJ10 in MDCK-wt or MDCK-Gc cells for five passages. For each seed, we compared their amino acid polymorphisms in HA with those in the associated fifth passage from both cells. Compared to the seed, rgCk/ WX13 gained polymorphisms in MDCK-Gc at residues 135 (A to A/T), 160 (changes in A/T ratio), 219 (A to A/E), 224 (D/N to D), and 250 (A to A/T), whereas rgMall/NJ10 acquired polymorphisms in MDCK-wt at residues 144 (G to G/D), 193 (K to K/T), and 225 (G to G/E) (Table 2). Interestingly, in MDCK-Gc (but not MDCK-wt), both viruses acquired adaptive substitutions at residues 461-471 of the fusion domain, although the changes in amino acids were not identical. Overall, rgCk/WX13 exhibited a higher number of polymorphisms in MDCK-Gc compared to MDCK-wt, whereas rgMall/NJ10 had an increase in polymorphisms in MDCK-wt compared to MDCK-Gc (Fig. 3b). These findings are consistent with a prior study that demonstrated human seasonal H1N1 and H3N2 IAVs, which bind exclusively to Neu5Ac, developed adaptive HA mutations when passaged in MDCK cells expressing Neu5Gc (17). Conversely, an enzootic canine H3N2 IAV, which binds to both Neu5Gc and Neu5Ac, did not exhibit significant HA mutations under the same conditions.

We further compared the viral infectious titers for the first and fifth passages using MDCK-wt cells. Results showed that rgCk/WX13 maintained similar titers after five passages in MDCK-wt cells (first passage: 1×10^7 TCID50/mL; fifth passage: 4.65×10^6 TCID50/mL), and rgMall/NJ10 exhibited a similar pattern when passaged five times in MDCK-Gc cells (first passage: 3.16×10^6 TCID50/mL; fifth passage: 4.65×10^6 TCID50/mL). However, when rgCk/WX13 was grown in MDCK-Gc cells, the fifth passage titer increased 2.15-fold (first passage: 1×10^7 TCID50/mL; fifth passage: 2.15×10^7 TCID50/mL), and rgMall/NJ10 increased 31.62-fold when adapting in MDCK-wt cells (first passage: 1×10^6 TCID50/mL; fifth passage: 3.16×10^7 TCID50/mL). These patterns support that the adaptive mutations in rgCk/WX13 enhanced its replication ability in MDCK-Gc cells,

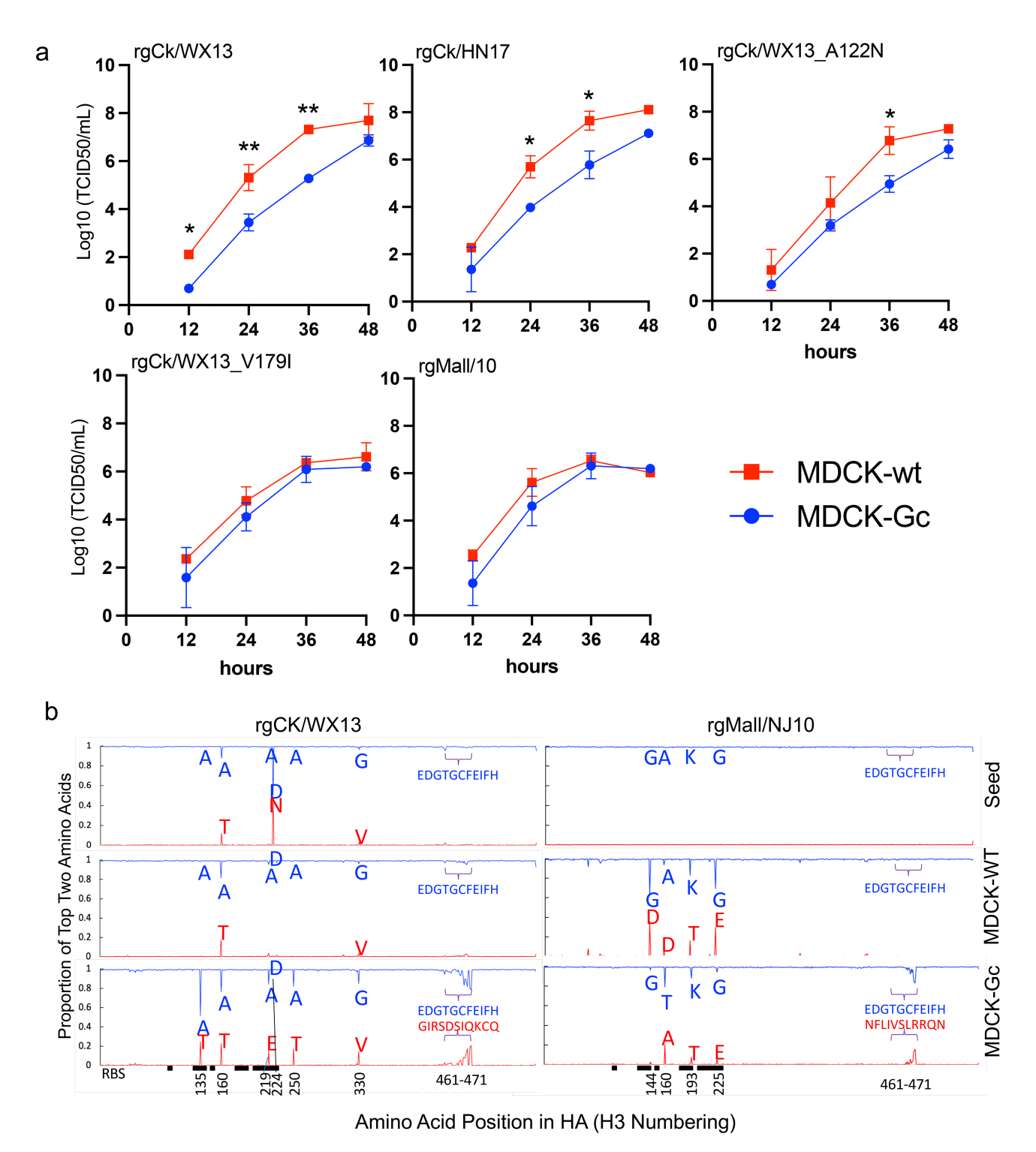


FIG 3 Neu5Gc affects virus replication of AH/13-lineage H7N9 viruses and drives adaptive mutations in the HA protein. (a) Growth kinetics of H7 influenza A viruses and mutants in MDCK-wt and MDCK-Gc cells. All viruses had HA genes from H7 viruses and the other seven from PR8, and three mutants were generated using the HA gene of Ck/WX13 as a template. Supernatants were collected at 12, 24, 48, and 72 hours post-infection and titrated by 50% tissue culture infection dose (TCID50) in MDCK CCL-34 cells. Two-way repeated measures analysis of variance were used to compare time-course growth data of H7 viruses among different cells. Statistical comparisons were shown as follows: not significantly different from n.s. (*P* > 0.05); *P* ≤ 0.05 as *; *P* < 0.01 as ***; *P* < 0.001 as ****; and *P* < 0.0001 as *****. (b) HA amino acid polymorphisms were detected in the seed viruses and the viruses from the fifth passage in MDCK-wt and MDCK-Gc cells. The viruses rgCk/WX13 and rgMall/NJ10, respectively, and other seven genes from PR8 were passaged five times in MDCK-wt and MDCK-Gc cells. The two most abundant non-synonymous mutations in the HA protein were plotted to visualize adaptive amino acid substitutions caused by cell passages. The location of the RBS in the HA protein was marked as a black bar. The predominant variant is highlighted in blue and the minor variant in red.

 $\textbf{TABLE 2} \quad \text{Amino acid polymorphisms in the HA protein for H7 viruses passaged in MDCK-wt and MDCK-Gc cells}^{a}$

Position (H3 numbering)	Virus						
	rgCk/WX13			rgMall/NJ10			
	SEED	MDCK-WT (P5)	MDCK-GC (P5)	SEED	MDCK-WT (P5)	MDCK-GC (P5)	
98 (RBS)	Υ	Υ	Υ	Υ	Υ	Υ	
34 (RBS)	G	G	G	G	G	G	
135 (RBS)	Α	T (87.39)	A (51.49)	Α	Α	Α	
		A (12.20)	T (24.91)				
36 (RBS)	T	T	T	T	T	T	
37 (RBS)	S	S	S	S	S	S	
38 (RBS)	Α	Α	Α	Α	Α	Α	
44	G	G	G	G	G (63.80) D (35.70)	G (96.37) D (3.07)	
53 (RBS)	W	W	W	W	W	W	
60 (RBS)	A (87.39)	A (70.75)	A (76.63)	Α	A (93.24)	T (78.75)	
,	T (12.20)	T (29.01)	T (23.15)		D (5.63)	A (20.73)	
83 (RBS)	H	H	Η	Н	Н	H	
88 (RBS)	T	T	T	A	A	A	
89 (RBS)	A	A	A	T	T	T	
	E	E		E	E	E	
90 (RBS)			E				
91 (RBS)	Q	Q	Q T	Q T	Q	Q	
92 (RBS)	T	T	T	T	T (82.68)	T (97.62)	
93 (RBS)	K	K	K	K	K (82.68) T (16.44)	K (87.62) T (7.81)	
94 (RBS)	L	L	L	L	L	L	
95 (RBS)	Y	Y	Y	Y	Y	Y	
10 (219)	A	A (83.65)	A (84.22)	A	A	A	
210 (219)	,,	E (15.30)	E (15.61)	,,	,,	,,	
21 (RBS)	Р	P	P	Р	Р	Р	
22 (RBS)	Q	Q	Q	Q	Q	Q	
23 (RBS)	V	V	V	V	V	V	
24 (RBS)	V D	N	v N	N	N	N	
25 (RBS)	G	G	G	G	G (68.94)	G (93.96)	
23 (ND3)	G	d	G	d	E (30.11)	E (5.55)	
26 (RBS)	L	L	L	Q	Q	Q	
27 (RBS)	S	S	S	S	S	S	
28 (RBS)	G	G	G	G	G	G	
41 (250)	A	A	A (81.98)	A	A	A	
(230)			T (17.66)				
22 (330)	G (96.40) V (3.28)	G	G (84.71)	G	G	G	
\===/	= (= =:==) . (5:20)	-	V (14.65)	-	-	-	
53 (461)	E	E	E (82.94)	Е	E	E	
,	-	_	G (7.74)	_	_	_	
54 (462)	D	D	D (89.99)	D	D	D (95.95)	
J-1 (TUL)	D	D	l (7.77)	U	D	F (2.91)	
EE (462)	C	c		G	G		
55 (463)	G	G	G (88.88)	G	G	G	
FC (ACA)	T	т.	R (10.74)	-	т.	T (05 50)	
56 (464)	Т	Т	T (85.30)	Т	Т	T (96.50)	
(445)			S (13.96)			I (13.32)	
57 (465)	G	G	G (81.79)	G	G	G (91.75)	
			D (17.47)			V (5.61)	
58 (466)	C	C	C	C	С	C (97.34)	
						S (1.29)	
59 (467)	F	F	F (97.86)	F	F	F (93.55)	

(Continued on next page)

TABLE 2 Amino acid polymorphisms in the HA protein for H7 viruses passaged in MDCK-wt and MDCK-Gc cells^a (Continued)

Position (H3 numbering)	Virus					
	rgCk/WX13			rgMall/NJ10		
	SEED	MDCK-WT (P5)	MDCK-GC (P5)	SEED	MDCK-WT (P5)	MDCK-GC (P5)
			I (8.46)			L (2.94)
460 (468)	E	E (79.86)	E	Е	E	E (96.55)
		Q (18.45)				R (2.78)
461 (469)	I	I (79.64)	1	1	I	I (84.64)
		K (19.59)				R (13.29)
462 (470)	F	F (78.60)	F	F	F	F (83.29)
		C (20.77)				Q (14.26)
463 (471)	Н	Н	Н	Н	Н	H (82.98)
						N (15.87)

The positions with <98% predominance for a single amino acid were listed in parenthesis, and the predominant amino acids are highlighted in bold. RBS, receptor binding sites.

potentially gaining Neu5Gc binding ability, while those in rgMall/NJ10 increased its replication ability in MDCK-wt cells, potentially losing Neu5Gc binding ability.

Taken together, the expression of Neu5Gc hinders replication of H7 viruses that exclusively bind to Neu5Ac but does not affect those that bind to both Neu5Ac and Neu5Gc, supporting our hypothesis. In addition, Neu5Gc expression creates a selective pressure that facilitates the acquisition of adaptive substitutions in H7 IAVs, particularly in residues within or near the HA RBS, enhancing virus replication in the cells.

Distribution of Neu5Gc in the respiratory and gastrointestinal tract tissues of chicken, wild Canada goose, and selected wild dabbling duck species

To investigate Neu5Gc expression patterns in chicken, wild Canada goose, and selected wild dabbling duck species, we conducted immunofluorescence (IF) staining using a Neu5Gc-specific antibody on formalin-fixed tissues from selected avian species. We examined the trachea, small intestine (duodenum/jejunum), and large intestine (colon and cloaca) of chicken, wild Canada goose (*Branta canadensis*), and five commonly surveyed wild dabbling ducks in North American IAV surveillance: mallard, gadwall (*Mareca strepera*), green-winged teal (*Anas carolinensis*), northern shoveler (*Spatula clypeata*), and wood duck (*Aix sponsa*). Results showed distinct Neu5Gc expression patterns between the species tested (Fig. 4). Neu5Gc expression was detected in mallard, green-winged teal, northern shoveler, and wood duck. In contrast, domestic chicken, Canada goose, and gadwall displayed no positive staining (Fig. 4a). Among the species with positive immunostaining, Neu5Gc expression was detected in the ciliated epithelial cells of the trachea and crypt cells within the duodenum/jejunum, colon, and cloaca (Fig. 4b). Notably, the northern shoveler exhibited significant Neu5Gc expression in the trachea, a pattern not observed in the other tested species.

In conclusion, Neu5Gc expression was absent in tissues tested from chicken, wild Canada geese, and gadwall, and was variable across the other wild duck species tested. Our previous study, utilizing Sambucus nigra agglutinins and Maackia amurensis lectin II binding assays, has revealed that all these testing species express Neu5Ac through their tracheal and gastrointestinal tissues. However, the distribution patterns of Neu5Ac α 2-3Gal and Neu5Ac α 2-6Gal varied among the species tested and their respective tissues (18).

A model proposed for H7 IAV adaptation and subsequent transmission upon spillover from wild waterbirds to gallinaceous poultry

This study demonstrates that AH/13-lineage H7N9 viruses in gallinaceous poultry, particularly chickens, bind exclusively to Neu5Ac, whereas H7 IAVs enzootic in wild waterbirds show binding affinities to both Neu5Gc and Neu5Ac. Strikingly, like the AH/13-lineage H7N9 viruses, all three H7 viruses responsible for recent epizootics in

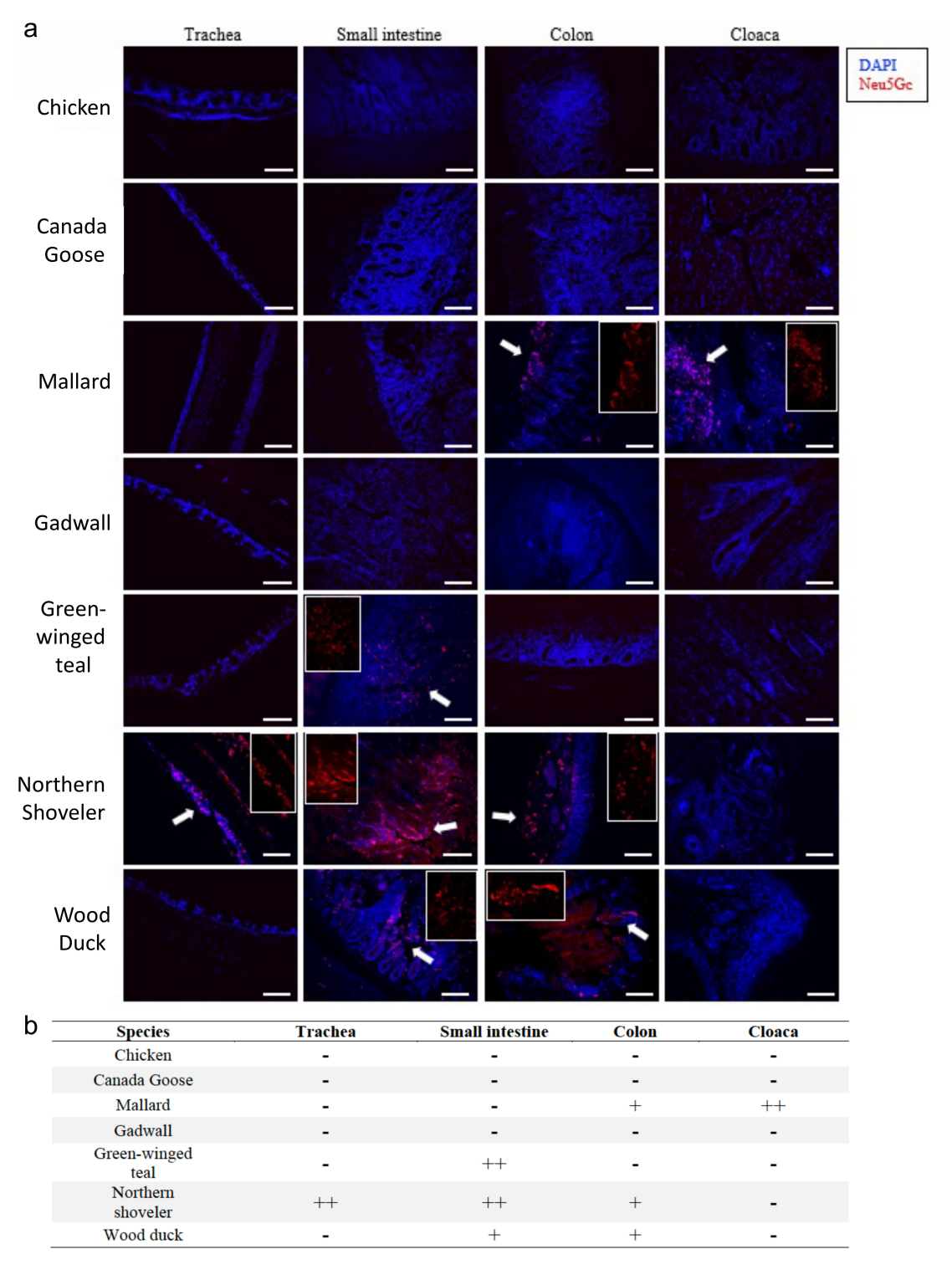


FIG 4 Distribution Neu5Gc glycan in the tissues of chicken, wild dabbling ducks, and Canada goose (*B. canadensis*). (a) The trachea, small intestine (duodenum/jejunum), colon, and cloaca of chicken (*Gallus gallus*), Canada goose, mallard (*A. platyrhynchos*), gadwall (*M. strepera*), green-winged teal (*A. carolinensis*), northern shoveler (*S. clypeata*), and wood duck (*A. sponsa*). Glycan terminated with Neu5Gc (red) was detected by immunofluorescence assay with an anti-Neu5Gc polyclonal antibody. Nuclei were stained with DAPI (blue). The white arrows indicated positive staining of Neu5Gc, the areas of which have been enlarged at the side of each image. The scale bar at the bottom of each image was 100 µm. (b) The abundance of Neu5Gc expression. We categorized the glycan receptor abundance: none or limited staining (−) without stained cells, moderate and sporadic staining (+) with <30% of stained cells, and strong staining (++) with ≥30% of the stained cells.

gallinaceous poultry also bind solely to Neu5Ac but not to Neu5Gc (16, 19, 20). These three outbreaks are H7N1 in the chicken population of Italy (1999–2000), H7N7 in the chicken population of the Netherlands (2003), and H7N3 in the chicken population of Mexico (2012–2013). By combining the findings on virus receptor binding specificity and host Neu5Gc expression, we propose a model for H7 IAV spillover from wild waterbirds to gallinaceous poultry (Fig. 5) and the potential evolutionary impact on subsequent transmission. An H7 IAV, with binding ability to both Neu5Gc and Neu5Ac, can be transmitted efficiently among waterbird species possessing both receptors. This virus may spill over into gallinaceous poultry. Once spillover occurs, a virus may acquire specific adaptive mutations in the HA protein and then lose Neu5Gc binding specificity (with the exclusive Neu5Ac binding ability). Consequently, the transmission capability of

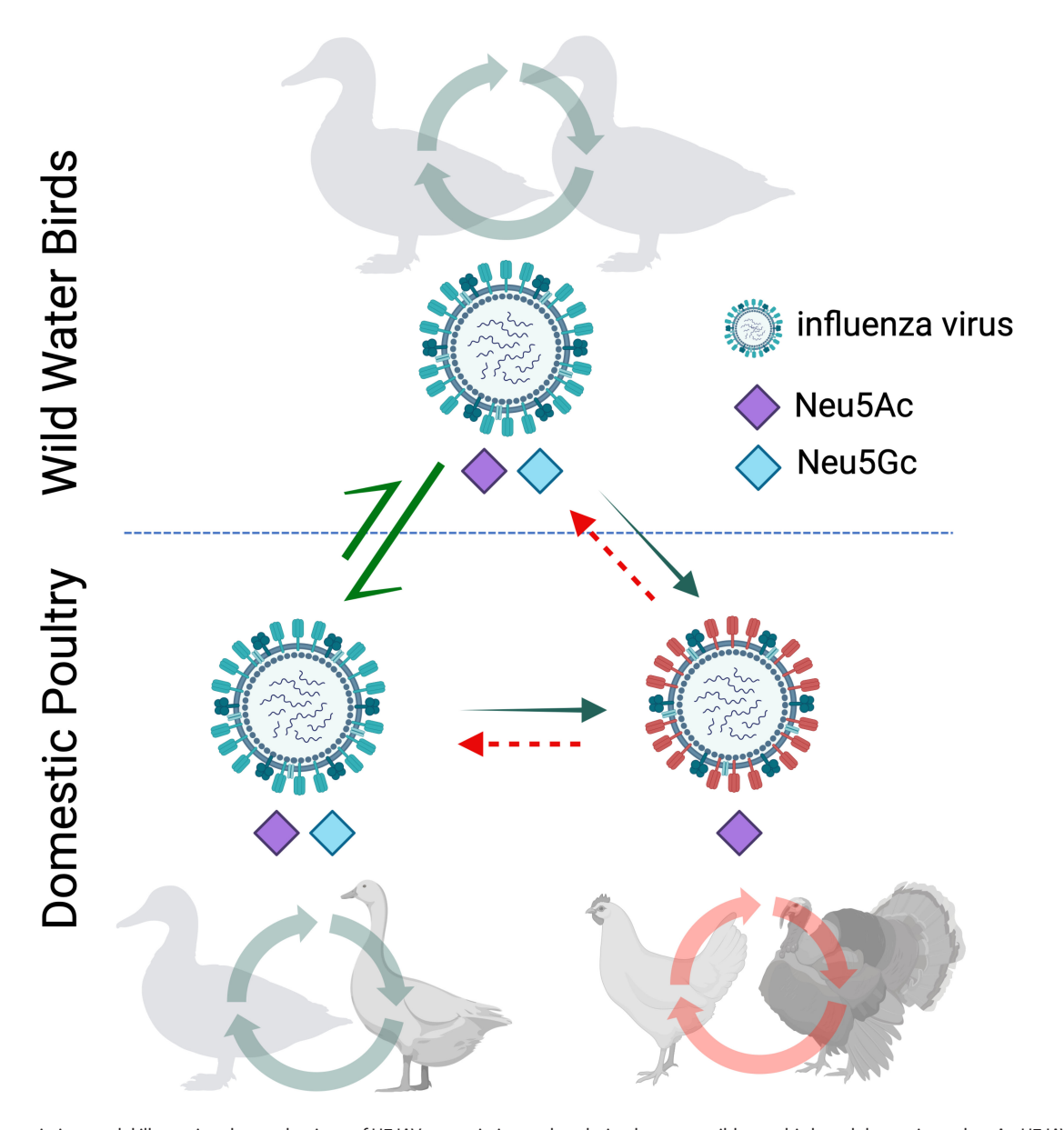


FIG 5 A transmission model illustrating the mechanisms of H7 IAV transmission and evolution between wild waterbirds and domestic poultry. An H7 IAV capable of binding to sialic acid receptors containing either Neu5Gc or Neu5Ac can be transmitted among wild waterbirds possessing these receptors, and can also transit between wild and domestic waterbirds expressed with the same receptors. This virus may then spill over into domestic poultry species (or another wild bird species) that express only Neu5Ac. Subsequent to this, the virus could acquire adaptive amino acid substitutions in the HA protein, leading it to lose its Neu5Gc binding ability and exclusively bind to Neu5Ac. Consequently, the transmission capability of these adapted viruses in waterbirds decreases. The figure was created by using BioRender.

these poultry-adapted viruses increases for gallinaceous poultry but decreases for wild waterbirds that possess both receptors. Further investigation is warranted to determine whether loss of Neu5Gc binding specificity can also occur for other subtypes of IAVs, including H5, and to understand whether Neu5Gc expression variations can restrict the transmission and adaption of IAVs among waterbirds, e.g., between those species with Neu5Gc expression and those without.

DISCUSSION

A wide variety of IAVs circulate among wild waterbirds, including migratory waterfowl, gulls, and shorebirds, and occasionally transmit to domestic poultry. However, these waterbird-origin viruses typically have poor replication efficiency in gallinaceous poultry (21). While all avian species share the SA2-3Gal receptor, this alone cannot explain the species barriers between waterbirds and gallinaceous poultry based on receptor binding. Among all IAVs, H7 viruses are one of the most commonly identified subtypes and are often isolated from migratory waterfowl, in particular dabbling ducks, diving ducks, shorebirds, geese, and swans (Fig. S1) (1). This study demonstrates that wild-type H7 viruses tested from wild waterbirds have glycan binding preferences for both Neu5Gc and Neu5Ac, while those that have undergone sustained transmission in gallinaceous poultry, particularly chickens, have lost the ability to bind Neu5Gc (Fig. 1). The absence of Neu5Gc expression in chickens exerts selective pressure on waterbird-origin H7 viruses, facilitating the acquisition of adaptive HA substitutions (19), such as I179V. Such adaptive substitutions result in the loss of Neu5Gc binding, enhance virus replication in Neu5Gc-free cells (Fig. 3), may have increased virus transmissibility in chickens (7), and consequently have led to the low detection rate of AH/13-lineage virus in domestic ducks during surveillance (12, 13). It would be useful to ascertain the point at which substitutions leading to the loss of Neu5Gc binding ability occur. This knowledge will enable timely interventions, such as depopulation, rather than resorting to controlled marketing (i.e., the strategic regulation of poultry sales and distribution), using this as an indicator (as illustrated in Fig. 5).

IAVs have large variations in binding avidities to Neu5Gc and Neu5Ac (22, 23), and most duck and gull origin IAVs from different subtypes including H1–H6, H9, and H11–H14 exhibited binding preference both to Neu5Gc and Neu5Ac but with stronger binding avidity to Neu5Gc (24). Thus, further studies are required to fully comprehend how Neu5Gc expression influences viral evolution and transmission of other subtypes of IAVs, particularly H5, among avian species, which could inform the development of more effective prevention and control measures against the spread of IAVs.

Compared to their precursor viruses from wild birds, the NA of the AH/13-lineage H7N9 virus exhibits a five-amino acid deletion at positions 69-73 (Gln-Ile-Ser-Asn-Thr), in addition to those changes in the HA described in this study. It is worth noting that similar deletions in the NA stalk region, albeit of varying lengths, have been observed in other poultry-adapted viruses, such as H7N1 in Italy (25), various H7N2 detected in the United States (26), and panzootic Goose/Guangdong/1996-like H5N1 viruses (27, 28). Previous studies have shown that NA stalk deletions in H2N2 viruses can enhance replication in chickens, suggesting a potential role for the deletion in the NA stalk of H7N9 in its adaptation to domestic poultry. Further experiments are needed to confirm this role and investigate the potential interplay between these genetic changes in facilitating the adaptation and transmission of AH/13-lineage H7N9 in gallinaceous poultry.

Infections caused by IAVs of subtypes H5 and H7 are listed as notifiable diseases, when detected in domestic poultry, by the World Organization for Animal Health due to the potential for these viruses to exhibit high pathogenicity among domestic poultry (29). Although national programs are in place to control avian influenza in poultry worldwide, measures such as active and passive surveillance of poultry and wild birds, poultry vaccination, and stamping out of positive cases among domestic flocks, have not always achieved eradication among domestic birds (29). Similar to many other cases, the AH/13-lineage H7N9 virus emerged as a low pathogenic avian influenza virus causing

minor clinical disease in chicken and ducks, the predominant poultry species in China (30). However, despite causing only mild symptoms in poultry, these viruses led to a high mortality rate of over 30% in humans (3). This AH/13-lineage H7N9 virus was identified as a novel reassortant between a wild bird-origin H7 virus and the H9N2 virus epizootic in domestic poultry, and molecular clocking showed that this virus had been circulating in poultry for at least a year before detection (15). This is further supported by the widespread distribution of this AH/13-lineage H7N9 virus in domestic poultry, particularly in live poultry markets, when the first human case of H7N9 infection was reported (31). The extended period of virus circulation likely allowed the AH/13-lineage H7N9 virus to adapt to domestic poultry, resulting in the emergence of Neu5Ac-specific binding preferences (Fig. 1) and increased transmission efficiency in gallinaceous poultry (7). These adapted AH/13-lineage H7N9 viruses rapidly became epizootic in eastern and southeastern China, evolving into multiple regionally distinct lineages with different reassortant genotypes (12, 32). The AH/13-lineage H7N9 virus evolved into a highly pathogenic form in 2017 and retained its high infectivity in gallinaceous poultry (13). Our findings indicate that the highly pathogenic variant of this virus maintained its Neu5Ac-specific binding preference (Fig. 1). Chinese Minister of Agriculture initiated the H5/H7 bivalent inactivated vaccination campaign in September 2017, resulting in a 93.3% decrease in the isolation rate of the H7N9 virus in poultry and eliminating human

In the United States, stamping out has been the primary method for controlling avian influenza viruses among domestic birds, and this method has successfully controlled all introductions of H7 IAVs into poultry during the past 10 years (34). We explored genomic polymorphisms of H7 isolates from eight spillover cases in US poultry (n = 18) and wild dabbling ducks (n = 85) (Table S3), and the results indicated that H7 viruses detected in US poultry exhibited more amino acid polymorphisms compared to those found in wild dabbling ducks (Fig. S3). However, it is important to note that only a small subset of these polymorphisms led to substitutions at the amino acid level (Table S4). Notably, two out of 18 isolates exhibited the key adaptive substitution V179I; and yet, all of the strains maintained their ability to bind to both Neu5Gc and Neu5Ac, suggesting that they had not fully adapted to the domestic poultry host (Fig. S3b and c). These results imply that the prompt implementation of stamping-out policies has likely been effective in preventing the emergence of poultry-adapted H7 strains. Thus, strict implementation of early detection and control policies may be crucial in minimizing the possibility of viral adaptation in poultry. That is, by promptly detecting and eliminating low pathogenicity avian influenza before they have the chance to adapt to domestic poultry, the risk of enzootic outbreaks, including potential highly pathogenic avian influenza outbreaks, can be significantly reduced.

In addition to avian species, H7s have sporadically caused infections in other mammals such as horses, harbor seals (35–37), and swine (37); some have been reported in humans as well (35, 38-46). Several previous reports support that Neu5Gc binding affects virus replication in mammals with Neu5Gc expression, although the role of Neu5Gc expression was not fully defined. For example, virus binding to Neu5Gc is a feature of IAVs that replicate in horses (47), and both an avian-origin H3N2 and an equine-origin H3N8 IAV acquired W222L, which leads to an increase in the binding affinity to Neu5Gc and enhances virus infection in canines (48, 49). On the other hand, given the H7 virus's ability to bind to human-like 6'SLN receptors (as shown in Fig. 1), the loss of Neu5Gc binding could potentially increase viral infectivity in humans that express only Neu5Ac, not Neu5Gc, in their respiratory tracts (50). At the interface of poultry and humans, the adaptation of H7 viruses to gallinaceous poultry further enhanced virus transmission ability and contributed to epizootic spread within domestic poultry populations, and such adaptation likely led to increased viral loads, consequently creating more opportunities for human exposures to the virus. Both factors likely contribute to the rise in human cases in these H7 outbreaks, such as H7N7 in the Netherlands (10) and H7N9 in China (3).

Our study on adaptive pressure demonstrated that Neu5Gc expression influences the evolution of H7 viruses, leading to adaptive amino acid substitutions in the RBD of the HA protein. Notably, we observed distinct amino acid changes depending on the presence or absence of Neu5Gc expression. Specifically, in the absence of Neu5Gc expression, the wild-type viruses (rgMall/NJ10) acquired polymorphisms at residues 144 (G to G/D), 193 (K to K/T), and 225 (G to G/E) and increased itstheir replication ability in MDCK-wt cells, potentially losing Neu5Gc binding ability. Conversely, in the presence of Neu5Gc expression, rgCk/WX13 gained polymorphisms in MDCK-Gc at residues 135 (A to A/T), 160 (with changes in the A/T ratio), 219 (A to A/E), 224 (D/N to D), and 250 (A to A/T) and enhanced its replication ability in MDCK-Gc cells, potentially gaining Neu5Gc binding ability. Interestingly, while positions 135, 160, and 193 overlapped those observed in the AH/13-lineage H7N9, other adaptive mutations observed in these MDCK cells differed from those observed in the AH/13-lineage H7N9 (Fig. 2). One possible contributing factor to this discrepancy is that the reverse genetics system may not accurately represent the quasispecies present in the virus population within birds. In addition, cell type may contribute to this variation, and further studies are warranted to investigate the role of Neu5Gc expression when using avian cells.

The enzyme cytidine monophospho-N-acetylneuraminic acid hydroxylase (CMAH) converts Neu5Ac to Neu5Gc. Some mammals such as horses, dogs, and pigs appear to maintain CMAH function and predominantly express Neu5Gc in various tissues (48, 51-53) (including the respiratory tract epithelium) (47), whereas humans and some mammals (such as seals) have lost CMAH function and do not express Neu5Gc (48, 54, 55). Genomic analyses have shown that all birds lack CMAH homologs (55), and Neu5Gc expression has not been detected in the muscle tissues in chicken, emu, and parrots; however, CMAH homologs have been detected in the liver or eggs of some avian species, possibly acquired from the diet or via an alternative pathway (56). Through an immunofluorescence assay, we demonstrated that Neu5Gc expression was widely present in the gastrointestinal tissues, such as cloaca and colon, of selected wild dabbling ducks, including mallard, green-winged teal, northern shoveler, and wood ducks, but not those of chickens (Fig. 4), which is consistent with a prior report that Neu5Gc was expressed in the intestines of Pekin ducks (Anas platyrhynchos domesticus) and mallards, mainly on the crypt epithelial cells of the colon (22). In addition to the gastrointestinal tracts, Neu5Gc expression was also observed in the respiratory tract tissues of the green-winged teal. Interestingly, neither the gastrointestinal nor the respiratory tracts of the gadwall or Canada goose showed Neu5Gc expression. One potential limitation is that our Neu5Gc expression analyses were based on a group of wild bird populations we sampled, and further study is needed to evaluate whether samples representing those polymorphisms in these wild birds have consistent Neu5Gc expression levels across these tissues. Future research is needed to investigate Neu5Gc expression in other avian species, both wild and domestic, not included in this study, such as diving ducks, gulls and terns, snow geese, swans, sea ducks, shorebirds, and others that might serve as natural reservoirs for avian influenza viruses. Additional investigation is warranted to determine if Neu5Gc expression influences IAV transmission and adaptation between waterbird species that express Neu5Gc and those that do not.

MATERIALS AND METHODS

Data

As of 1 March 2023, a total of 2,651 HA genomic sequences of subtype H7 avian IAVs were obtained from the Influenza Research Database (http://www.fludb.org). The sequences were sorted by location on five continents (Africa, Asia, Europe, North America, Oceania, and South America), as well as by species category. The species were categorized as gallinaceous poultry (chicken and others), waterfowl (duck and others), and other avian species (Table S1).

Viruses and virus propagation

The study utilized 26 strains of IAVs, including eight genetic reassortants containing the HA gene of AH/13-lineage H7N9 viruses, and 18 wild type or genetic reassortant viruses associated with contemporary H7 viruses from wild birds or domestic poultry from both North America and Eurasia (Table 1). All viruses were propagated in 9-day-old specific pathogen-free embryonated eggs at 37°C for 72 hours. The resulting allantoic fluids were collected and used in growth kinetics and virus purification, or stored at -80° C until needed for analysis.

Cells

The MDCK cells (CCL-34) were obtained from the American Type Culture Collection. The wild-type MDCK NBL-2 cells (MDCK-wt) and the MDCK cells expressing CMAH (MDCK-Gc) were adapted from another study (17). The cells were maintained in Dulbecco's modified Eagle's medium (DMEM, Gibco, New York, USA) supplemented with 10% fetal bovine serum (FBS; Atlanta Biologicals, Lawrenceville, GA, USA) at 37°C under 5% CO₂.

Nucleotide extraction, PCR, quantitative reverse transcription-PCR, and genomic sequencing

Viral RNA was extracted from the allantoic fluid of embryonated chicken eggs or cell culture supernatants by using the GeneJET Viral DNA/RNA purification kit (Thermo Fisher Scientific, Waltham, MA). The RNA was subjected to cDNA synthesis using SuperScript III Reverse Transcriptase (Thermo Fisher Scientific, Waltham, MA) according to the manufacturer's instructions. PCR products of the full-length HA were generated using IAV-specific primers (57). The plasmids were then extracted with GeneJET Plasmid Miniprep Kit (Thermo Scientific, Rockford, IL). The PCR products and plasmid insertions were confirmed without unexpected mutations by using Sanger sequencing.

Gene synthesis, molecular cloning, and reverse genetics

The HA genes of AH/13-lineage H7N9 viruses (as listed in Table 1) were synthesized and cloned into the pHW2000 vector by Gene Universal Inc. (Newark, DE). Meanwhile, the HA genes of A/mallard/New Jersey/A00926089/2010 (H7N3), A/domestic duck/ West Virginia/A00140913/2008 (H7N3), and A/mute swan/Rhode Island/A00325125/2008 (H7N3) were cloned into the pHW2000 vector using a universal primer described elsewhere (57). To generate the reassortant viruses, a HA gene from an H7 virus and seven other gene segments from A/Puerto Rico/8/1934 (H1N1) (PR8) wereas included using reverse genetics (58) (see Table 1 for details). The nucleotide sequences of the HA gene in each rescued virus were confirmed without unexpected mutations by Sanger sequencing.

Site-directed mutagenesis

To identify the specific amino acid substitution responsible for the acquisition of viral binding avidity to a sialic acid glycan terminated with Neu5Gc, we utilized the HA gene of Ck/WX13 as a template to create a set of mutants by site-directed mutagenesis. These mutants included amino acid substitution A122N (H3 numbering), A135E, V179I, or K193R in HA protein. To generate a specific mutation in the HA gene of Ck/WX13, we used the Phusion Site-Directed Mutagenesis Kit (Thermo Scientific, Rockford, IL) with primers listed in Table S6. Prior to PCR amplification, the primers were treated with T4 Polynucleotide Kinase (Thermo Scientific, Rockford, IL) for 5' phosphorylation according to the manufacturer's instructions. The site-directed mutagenesis PCR amplification mixture consisted of 23.5 μ L of water, 10 μ L of 5× Phusion HF buffer, 1 μ L of dNTPs (10 mM), 5 μ L of each T4 Polynucleotide Kinase-treated primer (5 μ M), 0.5 μ L of Phusion hot start DNA polymerase (2 U/ μ L), and 5 μ L of HA plasmid of A/chicken/Wuxi/ 0405005/2013 (H7N9) (Ck/WX13) (1 μ m/ μ L). The PCR parameters used for site-directed

mutagenesis were as follows: one cycle at 98°C for 30 seconds, followed by 24 cycles at 98°C for 10 seconds, 69°C for 30 seconds, and 72°C for 2 minutes, followed by a final extension step at 72°C for 5 minutes. The PCR products were digested with 1 μL of FastDigest DpnI at 37°C for 15 minutes. The ligation reaction was performed at room temperature for 5 minutes after digestion. The ligation mixture contained 2 μL of PCR products, 2 μL of 5× rapid ligation buffer, 0.5 μL of T4 DNA ligase, and 5.5 μL of water. The ligation products (5 μL) were transformed into DH10B Competent Cells (Thermo Scientific, Rockford, IL) following the manufacturer's protocol. The plasmids were extracted and then used for virus rescue.

Virus purification

To prepare for biolayer interferometry and glycan microarray analyses, the viruses were purified using sucrose gradient ultracentrifugation. Briefly, allantoic fluids collected from eggs infected with the virus wasere first centrifuged by $4,000 \times g$ for 30 minutes to remove any cell debris. Any remaining cellular debris was then removed further by ultracentrifugation at 4°C for 30 minutes at $18,000 \times g$. The virions were subsequently pelleted by ultracentrifugation at 4°C for 90 minutes at $112,000 \times g$. The virus was then collected (a "milky" band at around 40% sucrose) and pelleted again after sucrose gradient ultracentrifugation with four layers (30%, 40%, 50%, and 60%). The purified virus was then stored at -80°C until it was ready for use.

Glycan microarray analyses

The 75 N-linked glycans (59) were printed on slides derivatized with N-hydroxysuccinimide (NHS), as described elsewhere (60). Each glycan was printed in six replicates in a subarray at a concentration of 100 pM in phosphate buffer (100 mM sodium phosphate buffer, pH 8.5). Prior to the assay, the slides were rehydrated in TSMW buffer (20 mM Tris-HCl, 150 mM NaCl, 2 mM CaCl₂, 2 mM MgCl₂, 0.05% Tween, pH 7.4) for 5 minutes. A 15 µL aliquot of 1.0 M sodium bicarbonate (pH 9.0) was added to 150 µL of purified virus, and the virus was incubated with 25 µg of Alexa Fluor 488 NHS Ester (succinimidyl ester; Invitrogen) for 1 hour at 25°C. After overnight dialysis to remove excess Alexa 488, the virus HA titer was checked, and the virus was bound to the glycan array. The labeled viruses were then incubated on the slide at 4°C for 1 hour, washed, and briefly centrifuged before being scanned with an InnoScan 1100 AL fluorescence imager (Innopsys, Carbonne, France). Mean relative fluorescent units (RFU) and standard deviation were calculated for six replicates per virus. A threshold of 500 RFU was set to determine the background signal.

Biolayer interferometry assay and data analyses

The virus receptor binding avidities were determined by a biolayer interferometry assay with an Octet RED instrument (Pall ForteBio, Menlo Park, CA). Two biotinylated glycan analogs (3'SLN: Neu5Acα2-3Galβ1-4GlcNAcβ) and 6'SLN: Neu5Acα2-6Galβ1-4GlcNAcβ) were purchased (GlycoTech, Gaithersburg, MD). Three biotinylated glycans Neu5Acα2-3Galβ1-4(Fucα1-3)GlcNAcβ (sLeX), Neu5Gcα2-3Galβ1-4GlcNAcβ (3'GLN), and Neu5Gcα2-3Galβ1-4(Fucα1-3)GlcNAcβ (GLeX) were synthesized as previously described using GlcNAcβ-Biotin as starting substrate (59). The glycans were preloaded onto streptavidin-coated biosensors at up to 0.3 µg/mL for 5 minutes in 1× kinetic buffer (Pall FortéBio, Menlo Park, CA). Each test virus was diluted to a final concentration of 100 pM with 1× kinetic buffer containing 10 μM oseltamivir carboxylate (American Radiolabeled Chemicals, St. Louis, MO) and zanamivir (Sigma-Aldrich, St. Louis, MO) to prevent cleavage of the receptor analogs by NA proteins of the influenza virus. The association was measured for 30 minutes at 25°C, as described elsewhere (61). To evaluate the binding ability of a virus, we used one high concentration of glycans (0.5 μM) with 100 pM viruses to record the endpoint binding response of 30 minutes at 25°C. The threshold for determining positivity in glycan binding was set using the binding response from the

negative control, which did not load the virus but phosphate-buffered saline (PBS) only. To quantify virus binding avidity, glycan concentrations ranging from 0.05 to 0.5 ug/mL were used. The obtained binding responses were normalized by dividing them by the highest response value obtained during the experiment. Binding curves were fitted using the binding-saturation method, which was implemented in GraphPad Prism 8 software (https://www.graphpad.com/scientific-software/prism/). Normalized response curves were used to calculate the fractional saturation (f) of the sensor surface, as described elsewhere (62). The 50% relative sugar loading concentration (RSL_{0.5}) is a measure used to quantify the binding avidity between a virus and a glycan. It is calculated at half the fractional saturation (f = 0.5) of the virus against glycan analogs. RSL_{0.5} ranges between 0 and 1, and the lower the RSL_{0.5}, the stronger the binding affinity between the virus and the glycan analog. Conversely, the higher the RSL_{0.5}, the weaker the binding affinity between the virus and the glycan analog.

Structural modeling

In this study, the HA protein structure of A/Anhui/1/2013(H7N9) (PDB ID 4BSE) with the receptor α2,6-SLN bound to its RBS was employed as the reference template. It's noteworthy that the HA protein sequence of A/Anhui/1/2013(H7N9) is 100% identical to that of the Ck/WX13 used in our study. For our analysis, the receptor was manually adjusted to produce an H7:Neu5Ac complex. To simulate the effect of V179 versus I179 on Neu5Ac binding, the valine at position 179 was converted to isoleucine using Coot (63). Following the removal of all other small molecules and glycans in the original data set, both the wild type and the V179I mutant underwent energy minimization with Phenix (utilizing Phenix.elbow and Phenix.geometry_minimization) (64). Refining both the wild type and mutant structures was pursued to eliminate any potential biases associated with the algorithm. For a comparative analysis, the two refined structures were aligned using Pymol (via the Pymol.align function) (The PyMOL Molecular Graphics System, Version 1.3, Schrödinger, LLC).

To model Neu5Gc binding to both wild type and V179I mutant from Ck/WX13, the Neu5Gc moiety from another previously solved H7 HA structure [PDB ID 7TIV, A/equine/NY/49/73 (H7N7)] was superimposed into the above-mentioned H7:Neu5Ac structure using Pymol. The resulting H7:Neu5Gc complex was subjected to V179I mutation, energy minimization, and comparative analysis using the same modeling procedures mentioned above.

All structural figures were prepared using Pymol (The PyMOL Molecular Graphics System, Version 1.3, Schrödinger, LLC).

Growth kinetics in Neu5Gc expressed MDCK cells

To evaluate the impact of Neu5Gc expression on virus infectivity of H7 viruses, we conducted growth kinetics analyses of three selected viruses (rgMall/NJ10, rgCk/WX13, and rgCk/HN17) on both MDCK-wt and MDCK-Gc. Additionally, we included two mutant viruses (A122N and V179I) in the growth kinetics analyses to assess whether each of these three amino acid substitutions may affect virus replication efficiency. To initiate infection, cells were seeded in 6-well plates and allowed to grow for approximately 18 hours, reaching 90% confluency. The cells were then infected with each testing virus at a multiplicity of infection of 0.001. Following infection, supernatants were collected at 12, 24, 36, and 48 hours post-infection and subjected to viral titration.

Viral titration

For viral titration, we determined the 50% tissue culture infection dose (TCID50) on MDCK CCL-34 cells. Briefly, cells were seeded at a density of 2×10^4 cells per well in a 96-well plate with Opti-MEM I Reduced Serum Medium. Cells were then incubated at 37°C with 5% CO $_2$ for 18–20 hours before virus inoculation. Viral samples were serially diluted in Opti-MEM I Reduced Serum Medium supplemented with 1 μ g/mL

of TPCK-trypsin. Subsequently, 200 μ L of each virus dilution was inoculated onto MDCK cells in quadruplicate. Infected cells were then incubated at 37°C with 5% CO₂ for 72 hours and evaluated for positivity using hemagglutination assays. The number of positive and negative wells for each dilution wereas recorded for TCID50 calculation based on the method described by Reed and Muench (65).

Hemagglutination assays

Hemagglutination assays were carried out by using 0.5% turkey erythrocytes as described elsewhere (66).

Characterization of adaptative mutations on cells

To investigate the effects of Neu5Ac and Neu5Gc on the adaptive mutations, we passaged rgCk/WX13 and rgMall/NJ10 in MDCK-wt and MDCK-Gc cells five times. For each passage, the original seed virus or supernatants were diluted 200-fold during the virus infection. Viral RNA was extracted from the seed virus and supernatants from the fifth passage and subjected to next-generation sequencing.

Next-generation sequencing, genomic assembly, and polymorphism analyses

Conventional two-step reverse transcription-PCR whole genome amplification was set up using eight pairs of universal primers (57). Viral RNA was reverse transcribed to cDNA using SuperScript III Reverse Transcriptase (ThermoFisher Scientific, Cat. #: 18080-044). PCR amplification was subsequently performed using Platinum Tag DNA Polymerase High Fidelity (ThermoFisher Scientific, Cat. #: 11304-102). Amplicons of the same samples were pooled together before purification. AMPure XP beads (Beckman Coulter, Cat. #: A63881) purified amplicons were analyzed for cDNA quality and quantity using TapeStation 4200 (Agilent Technologies, Santa Clara, CA) DNA5000 kit (Agilent Technologies, Cat. #: 5067-5588, 5589).

After TapeStation analysis, ~50 ng of pooled cDNA of each sample was used as input for library preparation using an Illumina DNA prep kit (Illumina, Cat. # 20018705) following the manufacturers' instructions. The purified libraries with different indexes were quantitated using a TapeStation D5000 kit and equal molars of each library were pooled together. Pooled libraries were denatured, diluted to an appropriate loading concentration, and loaded onto a Miseq 600 cycles V3 cartridge (Illumina, Cat. #: MS-102-3003) for sequencing.

Iterative Refinement Meta-Assembler v.1.0.3 (https://wonder.cdc.gov/amd/flu/irma/) was used for sequence assembly and nucleotide variant analysis, and the results were further validated by CLC Genomics Workbench v21.0.3. The quality of the reads was trimmed with a Phred quality score of 20, which indicates a base call accuracy of 99%, the likelihood of finding one incorrect base call among 100 bases. The polymorphisms were analyzed by using DiversiTools (http://josephhughes.github.io/DiversiTools/). The most abundant non-synonymous mutations in HA protein were plotted to visualize adaptive amino acid substitutions caused by cell passages.

To identify the intra-host genetic diversity of H7 viruses, the minor amino acid variants ratio was calculated by the sum of the second and third amino acid counts divided by the sum of the top three amino acid counts in each residue. Ggplot R package was used for amino acid variants visualization. To minimize the impacts of potential sequence errors on the intra-host variant analyses, only those amino acid variants ratios with >5% were considered.

Multiple sequence alignment and phylogenetic analyses

Multiple sequence alignments were generated using Muscle v5.1 (67). The approximately-maximum-likelihood phylogenetic tree was inferred by using fastTree v 2.1.11

(68). Phylogenetic trees were visualized by using FigTree v1.4.3 (http://tree.bio.ed.ac.uk/software/figtree/).

Characterization of Neu5Gc expression in avian respiratory and gastrointestinal tracts

A total of seven species were studied in this study, including chicken (Gallus gallus), Canada goose (B. canadensis), mallard (A. platyrhynchos), gadwall (M. strepera), greenwinged teal (A. carolinensis), northern shoveler (S. clypeata), and wood duck (A. sponsa). The avian respiratory and gastrointestinal tract (cloaca and colon) tissues were collected and fixed by submerging them in 10% neutral buffered formalin, and then they were embedded in paraffin. Sections of 5 µm were made from the embedded tissues. The tissue sections were deparaffinized by dipping into the following solutions: three times of 10 minutes in xylene, 3 minutes of 100% ethanol, 100% ethanol, 95% ethanol, 70% ethanol, 50% ethanol, and rinsed in ddH₂O. Antigen was then heat-induced target retrieved with diluted Target Retrieval Solution, Citrate pH 6.1 (10x) following the manufacturer's manual (Dako, Carpinteria, CA). The sections were blocked by 3% Bovine Serum Albumin for 1 hour at room temperature. The sections were rinsed with PBS and incubated with the anti-Neu5Gc (1:500 dilution; Biolegend, San Diego, CA) overnight at 4°C. Sections were incubated with goat anti-chicken IgY (H+L) secondary antibody conjugated with Alexa Fluor 594 at 1:500 dilution with PBS before counterstaining with DAPI. The sections were washed three times offor 5 minutes with PBST after every step of antibody incubation. The slides were air -dried and covered with coverslips by using a Prolong antifade reagent. Images were captured with the Zeiss Axiovert 200M.

In our experiment, chicken and mallard colon tissues were used as negative and positive controls, respectively. Chicken, known for its lack of Neu5Gc expression and previously utilized in the generation of anti-Neu5Gc antibodies, served as the negative control (69). Conversely, mallard colon tissue, confirmed to express Neu5Gc (22), acted as the positive control. In our study, we included two or three individual animals from each species, contingent on their availability. Additionally, we repeated each staining procedure at least twice to ensure reliability.

Structural visualization

The HA protein was visualized in PyMOL using the template HA protein structure of A/Shanghai/02/2013 (H7N9) (accession number: 4LN3) from the Protein Data Bank (PDB, https://www.rcsb.org/).

Statistical analyses

A two-way analysis of variance test was performed using GraphPad Prism 8 (https://www.graphpad.com/scientific-software/prism/) to compare the statistical differences between viral titers at different time points in the growth kinetics of both the wild type and a testing mutant. A *P*-value of 0.05 was considered significant.

ACKNOWLEDGMENTS

We are thankful to Wendy S. Weichert for technical support and appreciate comments on prior drafts of the manuscript provided by Andrew Ramey. In addition, we thank Dennis Kohler and USDA wildlife disease biologists for providing wild bird samples. We would like to acknowledge the useful resource of the Influenza Research Database and the support from BEI resources.

This project was partially supported by the National Institutes of Health (grant numbers R21AI144433 and R01AI147640), the National Science Foundation (#2109745), and the Welch Foundation (C-1565 to Y.J.T.).

The findings and conclusions in this report are those of the authors and do not necessarily represent the official position of the U.S. Government.

AUTHOR AFFILIATIONS

¹Center for Influenza and Emerging Infectious Diseases (CIEID), University of Missouri, Columbia, Missouri, USA

²Department of Molecular Microbiology and Immunology, School of Medicine, University of Missouri, Columbia, Missouri, USA

³Bond Life Sciences Center, University of Missouri, Columbia, Missouri, USA

⁴US Department of Agriculture Animal and Plant Health Inspection Service, Fort Collins, Colorado, USA

⁵Department of Bioengineering, Rice University, Houston, Texas, USA

⁶Viral Diseases Branch, Walter Reed Army Institute of Research, Silver Spring, Maryland, USA

⁷Department of Chemistry and Center for Diagnostics and Therapeutics, Georgia State University, Atlanta, Georgia, USA

⁸National Veterinary Services Laboratories, Veterinary Services, U.S. Department of Agriculture, Ames, Iowa, USA

⁹Department of Pathobiology and Population Medicine, College of Veterinary Medicine, Mississippi State University, Mississippi State, Mississippi, USA

¹⁰Department of BioSciences, Rice University, Houston, Texas, USA

¹¹Department of Microbiology and Immunology, College of Veterinary Medicine, Baker Institute for Animal Health, Cornell University, Ithaca, New York, USA

¹²Department of Electrical Engineering and Computer Science, College of Engineering, University of Missouri, Columbia, Missouri, USA

AUTHOR ORCIDs

Minhui Guan http://orcid.org/0000-0003-3442-1068

Thomas J. DeLiberto http://orcid.org/0000-0003-1115-1472

Yizhi Jane Tao (1) http://orcid.org/0000-0002-0149-2241

Colin Parrish http://orcid.org/0000-0002-1836-6655

Xiu-Feng Wan http://orcid.org/0000-0003-2629-9234

FUNDING

Funder	Grant(s)	Author(s)
HHS NIH National Institute of Allergy and Infectious Diseases (NIAID)	R21Al144433	Xiu-Feng Wan
Welch Foundation (The Welch Foundation)	C-1565	Yizhi Jane Tao
National Science Foundation (NSF)	2109745	Xiu-Feng Wan
HHS NIH National Institute of Allergy and Infectious Diseases (NIAID)	R01AI147640	Xiu-Feng Wan

DATA AVAILABILITY

The raw and assembled genomic data collected from this study are available in GenBank with the BioProject accession number PRJNA978106. This submission includes six data sets (seed virus rgCk/WX13 and Mall/NJ10 and their corresponding fifth passages in MDCK-wt and MDCK-Gc), data sets for 85 H7 viruses from dabbling ducks, and 18 H7 viruses from domestic poultry from North America.

ETHICS APPROVAL

All experiments involving live viruses were performed in an approved biosafety level 2 (BSL-2) at the University of Missouri-Columbia, under protocol no. 19-09, in compliance with the Institutional Biosafety Committee of the University of Missouri-Columbia. Tissue samples from wild dabbling ducks and Canada geese were supplied by USDA/ APHIS Wildlife Services. Chicken tissue samples were obtained from a secondary-use

experiment (18), which was approved by the Institutional Animal Care and Use Committee of Mississippi State University (IACUC 17-719).

ADDITIONAL FILES

The following material is available online.

Supplemental Material

Supplemental tables and figures (JVI00119-24-s0001.pdf). Tables S1-S6; Fig. S1-S3.

REFERENCES

- Olsen B, Munster VJ, Wallensten A, Waldenström J, Osterhaus ADME, Fouchier RAM. 2006. Global patterns of influenza A virus in wild birds. Science 312:384–388. https://doi.org/10.1126/science.1122438
- Long JS, Mistry B, Haslam SM, Barclay WS. 2019. Host and viral determinants of influenza A virus species specificity. Nat Rev Microbiol 17:67–81. https://doi.org/10.1038/s41579-018-0115-z
- Jiang W, Hou G, Li J, Peng C, Wang S, Liu S, Zhuang Q, Chen J, Liu H. 2019. Prevalence of H7N9 subtype avian influenza viruses in poultry in China, 2013-2018. Transbound Emerg Dis 66:1758–1761. https://doi.org/ 10.1111/tbed.13183
- Xiang N, Li X, Ren R, Wang D, Zhou S, Greene CM, Song Y, Zhou L, Yang L, Davis CT, et al. 2016. Assessing change in avian influenza A(H7N9) virus infections during the fourth epidemic - China, September 2015-August 2016. MMWR Morb Mortal Wkly Rep 65:1390–1394. https://doi.org/10. 15585/mmwr.mm6549a2
- Chen Y, Liang W, Yang S, Wu N, Gao H, Sheng J, Yao H, Wo J, Fang Q, Cui D, et al. 2013. Human infections with the emerging avian influenza A H7N9 virus from wet market poultry: clinical analysis and characterisation of viral genome. Lancet 381:1916–1925. https://doi.org/10.1016/S0140-6736(13)60903-4
- Wang C, Wang J, Su W, Gao S, Luo J, Zhang M, Xie L, Liu S, Liu X, Chen Y, Jia Y, Zhang H, Ding H, He H. 2014. Relationship between domestic and wild birds in live poultry market and a novel human H7N9 virus in China. J Infect Dis 209:34–37. https://doi.org/10.1093/infdis/jit478
- Pantin-Jackwood MJ, Miller PJ, Spackman E, Swayne DE, Susta L, Costa-Hurtado M, Suarez DL. 2014. Role of poultry in the spread of novel H7N9 influenza virus in China. J Virol 88:5381–5390. https://doi.org/10.1128/ IVI.03689-13
- 8. Millman AJ, Havers F, Iuliano AD, Davis CT, Sar B, Sovann L, Chin S, Corwin AL, Vongphrachanh P, Douangngeun B, Lindblade KA, Chittaganpitch M, Kaewthong V, Kile JC, Nguyen HT, Pham DV, Donis RO, Widdowson MA. 2015. Detecting spread of avian influenza A(H7N9) virus beyond China. Emerg Infect Dis 21:741–749. https://doi.org/10.3201/eid2105.141756
- Capua I, Mutinelli F, Marangon S, Alexander DJ. 2000. H7N1 avian influenza in Italy (1999 to 2000) in intensively reared chickens and turkeys. Avian Pathol 29:537–543. https://doi.org/10.1080/-03079450020016779
- Stegeman A, Bouma A, Elbers ARW, de Jong MCM, Nodelijk G, de Klerk F, Koch G, van Boven M. 2004. Avian influenza A virus (H7N7) epidemic in the Netherlands in 2003: course of the epidemic and effectiveness of control measures. J Infect Dis 190:2088–2095. https://doi.org/10.1086/ 425583
- Kapczynski DR, Pantin-Jackwood M, Guzman SG, Ricardez Y, Spackman E, Bertran K, Suarez DL, Swayne DE. 2013. Characterization of the 2012 highly pathogenic avian influenza H7N3 virus isolated from poultry in an outbreak in Mexico: pathobiology and vaccine protection. J Virol 87:9086–9096. https://doi.org/10.1128/JVI.00666-13
- Lam TT-Y, Wang J, Shen Y, Zhou B, Duan L, Cheung C-L, Ma C, Lycett SJ, Leung CY-H, Chen X, et al. 2013. The genesis and source of the H7N9 influenza viruses causing human infections in China. Nature New Biol 502:241–244. https://doi.org/10.1038/nature12515
- Shi J, Deng G, Kong H, Gu C, Ma S, Yin X, Zeng X, Cui P, Chen Y, Yang H, et al. 2017. H7N9 virulent mutants detected in chickens in China pose an increased threat to humans. Cell Res 27:1409–1421. https://doi.org/10. 1038/cr.2017.129

- Broszeit F, Tzarum N, Zhu X, Nemanichvili N, Eggink D, Leenders T, Li Z, Liu L, Wolfert MA, Papanikolaou A, Martínez-Romero C, Gagarinov IA, Yu W, García-Sastre A, Wennekes T, Okamatsu M, Verheije MH, Wilson IA, Boons G-J, de Vries RP. 2019. N-glycolylneuraminic acid as a receptor for influenza A viruses. Cell Rep 27:3284–3294. https://doi.org/10.1016/j. celrep.2019.05.048
- Liu D, Shi W, Shi Y, Wang D, Xiao H, Li W, Bi Y, Wu Y, Li X, Yan J, Liu W, Zhao G, Yang W, Wang Y, Ma J, Shu Y, Lei F, Gao GF. 2013. Origin and diversity of novel avian influenza A H7N9 viruses causing human infection: phylogenetic, structural, and coalescent analyses. Lancet 381:1926–1932. https://doi.org/10.1016/S0140-6736(13)60938-1
- Spruit CM, Zhu X, Tomris I, Ríos-Carrasco M, Han AX, Broszeit F, van der Woude R, Bouwman KM, Luu MMT, Matsuno K, Sakoda Y, Russell CA, Wilson IA, Boons G-J, de Vries RP. 2022. N-glycolylneuraminic acid binding of avian and equine H7 influenza A viruses. J Virol 96:e0212021. https://doi.org/10.1128/jvi.02120-21
- Barnard KN, Wasik BR, Alford BK, Hayward JJ, Weichert WS, Voorhees IEH, Holmes EC, Parrish CR. 2021. Sequence dynamics of three influenza A virus strains grown in different MDCK cell lines, including those expressing different sialic acid receptors. J Evol Biol 34:1878–1900. https: //doi.org/10.1111/jeb.13890
- Guan M, Olivier AK, Lu X, Epperson W, Zhang X, Zhong L, Waters K, Mamaliger N, Li L, Wen F, Tao YJ, DeLiberto TJ, Wan XF. 2022. The Sialyl lewis X glycan receptor facilitates infection of subtype H7 avian influenza A viruses. J Virol 96:e0134422. https://doi.org/10.1128/jvi. 01344-22
- Youk S, Leyson C, Killian ML, Torchetti MK, Lee DH, Suarez DL, Pantin-Jackwood MJ. 2022. Evolution of the North American lineage H7 avian influenza viruses in association with H7 virus's introduction to poultry. J Virol 96:e0027822. https://doi.org/10.1128/jvi.00278-22
- Yang H, Carney PJ, Donis RO, Stevens J. 2012. Structure and receptor complexes of the hemagglutinin from a highly pathogenic H7N7 influenza virus. J Virol 86:8645–8652. https://doi.org/10.1128/JVI.00281-12
- Bergervoet SA, Germeraad EA, Alders M, Roose MM, Engelsma MY, Heutink R, Bouwstra R, Fouchier RAM, Beerens N. 2019. Susceptibility of chickens to low pathogenic avian influenza (LPAI) viruses of wild birdand poultry-associated subtypes. Viruses 11:1010. https://doi.org/10. 3390/v11111010
- Ito T, Suzuki Y, Suzuki T, Takada A, Horimoto T, Wells K, Kida H, Otsuki K, Kiso M, Ishida H, Kawaoka Y. 2000. Recognition of N-glycolylneuraminic acid linked to galactose by the alpha2,3 linkage is associated with intestinal replication of influenza A virus in ducks. J Virol 74:9300–9305. https://doi.org/10.1128/jvi.74.19.9300-9305.2000
- Gambaryan AS, Matrosovich TY, Philipp J, Munster VJ, Fouchier RAM, Cattoli G, Capua I, Krauss SL, Webster RG, Banks J, Bovin NV, Klenk H-D, Matrosovich MN. 2012. Receptor-binding profiles of H7 subtype influenza viruses in different host species. J Virol 86:4370–4379. https://doi.org/10.1128/JVI.06959-11
- Gambaryan A, Yamnikova S, Lvov D, Tuzikov A, Chinarev A, Pazynina G, Webster R, Matrosovich M, Bovin N. 2005. Receptor specificity of influenza viruses from birds and mammals: new data on involvement of the inner fragments of the carbohydrate chain. Virology (Auckl) 334:276–283. https://doi.org/10.1016/j.virol.2005.02.003
- Banks J, Speidel ES, Moore E, Plowright L, Piccirillo A, Capua I, Cordioli P, Fioretti A, Alexander DJ. 2001. Changes in the haemagglutinin and the

neuraminidase genes prior to the emergence of highly pathogenic H7N1 avian influenza viruses in Italy. Arch Virol 146:963–973. https://doi.org/10.1007/s007050170128

- Spackman E, Senne DA, Davison S, Suarez DL. 2003. Sequence analysis of recent H7 avian influenza viruses associated with three different outbreaks in commercial poultry in the United States. J Virol 77:13399– 13402. https://doi.org/10.1128/jvi.77.24.13399-13402.2003
- Xu X, Subbarao K, Cox NJ, Guo Y. 1999. Genetic characterization of the pathogenic influenza A/Goose/Guangdong/1/96 (H5N1) virus: similarity of its hemagglutinin gene to those of H5N1 viruses from the 1997 outbreaks in Hong Kong. Virol (Auckl) 261:15–19. https://doi.org/10. 1006/viro.1999.9820
- Wan XF, Ren T, Luo KJ, Liao M, Zhang GH, Chen JD, Cao WS, Li Y, Jin NY, Xu D, Xin CA. 2005. Genetic characterization of H5N1 avian influenza viruses isolated in southern China during the 2003-04 avian influenza outbreaks. Arch Virol 150:1257–1266. https://doi.org/10.1007/s00705-004-0474-9
- Swayne DE, Pavade G, Hamilton K, Vallat B, Miyagishima K. 2011. Assessment of national strategies for control of high-pathogenicity avian influenza and low-pathogenicity notifiable avian influenza in poultry, with emphasis on vaccines and vaccination. Rev Sci Tech 30:839–870. https://doi.org/10.20506/rst.30.3.2081
- Zhang Q, Shi J, Deng G, Guo J, Zeng X, He X, Kong H, Gu C, Li X, Liu J, et al. 2013. H7N9 influenza viruses are transmissible in ferrets by respiratory droplet. Science 341:410–414. https://doi.org/10.1126/ science.1240532
- Li Y, Huang X-M, Zhao D-M, Liu Y-Z, He K-W, Liu Y-X, Chen C-H, Long L-P, Xu Y, Xie X-X, Han K-K, Liu X-Y, Yang J, Zhang Y-F, Fan F, Webby R, Wan X-F. 2016. Detection of avian H7N9 influenza A viruses in the yangtze delta region of china during early H7N9 outbreaks. Avian Dis 60:118–125. https://doi.org/10.1637/11098-042015-Reg
- Lam T-Y, Zhou B, Wang J, Chai Y, Shen Y, Chen X, Ma C, Hong W, Chen Y, Zhang Y, Duan L, Chen P, Jiang J, Zhang Y, Li L, Poon LLM, Webby RJ, Smith DK, Leung GM, Peiris JSM, Holmes EC, Guan Y, Zhu H. 2015. Dissemination, divergence and establishment of H7N9 influenza viruses in China. Nat New Biol 522:102–105. https://doi.org/10.1038/ nature14348
- Zeng X, Tian G, Shi J, Deng G, Li C, Chen H. 2018. Vaccination of poultry successfully eliminated human infection with H7N9 virus in China. Sci China Life Sci 61:1465–1473. https://doi.org/10.1007/s11427-018-9420-1
- Olsen SJ, Rooney JA, Blanton L, Rolfes MA, Nelson DI, Gomez TM, Karli SA, Trock SC, Fry AM. 2019. Estimating risk to responders exposed to avian influenza A H5 and H7 viruses in poultry, United States, 2014–2017. Emerg Infect Dis 25:1011–1014. https://doi.org/10.3201/eid2505. 181253
- Webster RG, Geraci J, Petursson G, Skirnisson K. 1981. Conjunctivitis in human beings caused by influenza A virus of seals. N Engl J Med 304:911. https://doi.org/10.1056/NEJM198104093041515
- Lang G, Gagnon A, Geraci JR. 1981. Isolation of an influenza A virus from seals. Arch Virol 68:189–195. https://doi.org/10.1007/BF01314571
- Kwon TY, Lee SS, Kim CY, Shin JY, Sunwoo SY, Lyoo YS. 2011. Genetic characterization of H7N2 influenza virus isolated from pigs. Vet Microbiol 153:393–397. https://doi.org/10.1016/j.vetmic.2011.06.011
- Banks J, Speidel E, Alexander DJ. 1998. Characterisation of an avian influenza A virus isolated from A human--is an intermediate host necessary for the emergence of pandemic influenza viruses? Arch Virol 143:781–787. https://doi.org/10.1007/s007050050329
- Campbell CH, Webster RG, Breese SS. 1970. Fowl plague virus from man. J Infect Dis 122:513–516. https://doi.org/10.1093/infdis/122.6.513
- DeLay PD, Casey HL, Tubiash HS. 1967. Comparative study of fowl plague virus and a virus isolated from man. Public Health Rep (1896) 82:615– 620
- 41. Kurtz J, Manvell RJ, Banks J. 1996. Avian influenza virus isolated from a woman with conjunctivitis. Lancet 348:901–902. https://doi.org/10.1016/S0140-6736(05)64783-6
- 42. Taylor HR, Turner AJ. 1977. A case report of fowl plague keratoconjunctivitis. Br J Ophthalmol 61:86–88. https://doi.org/10.1136/bjo.61.2.86
- Koopmans M, Wilbrink B, Conyn M, Natrop G, van der Nat H, Vennema H, Meijer A, van Steenbergen J, Fouchier R, Osterhaus A, Bosman A. 2004. Transmission of H7N7 avian influenza A virus to human beings during A

- large outbreak in commercial poultry farms in the Netherlands. Lancet 363:587–593. https://doi.org/10.1016/S0140-6736(04)15589-X
- 44. Fouchier RAM, Schneeberger PM, Rozendaal FW, Broekman JM, Kemink SAG, Munster V, Kuiken T, Rimmelzwaan GF, Schutten M, Van Doornum GJJ, Koch G, Bosman A, Koopmans M, Osterhaus A. 2004. Avian influenza A virus (H7N7) associated with human conjunctivitis and A fatal case of acute respiratory distress syndrome. Proc Natl Acad Sci U S A 101:1356–1361. https://doi.org/10.1073/pnas.0308352100
- Tweed SA, Skowronski DM, David ST, Larder A, Petric M, Lees W, Li Y, Katz J, Krajden M, Tellier R, Halpert C, Hirst M, Astell C, Lawrence D, Mak A. 2004. Human illness from avian influenza H7N3, British Columbia. Emerg Infect Dis 10:2196–2199. https://doi.org/10.3201/eid1012.040961
- Dudley JP. 2008. Public health and epidemiological considerations for avian influenza risk mapping and risk assessment. Ecol Soc 13. https:// doi.org/10.5751/ES-02548-130221
- Suzuki Y, Ito T, Suzuki T, Holland RE, Chambers TM, Kiso M, Ishida H, Kawaoka Y. 2000. Sialic acid species as A determinant of the host range of influenza A viruses. J Virol 74:11825–11831. https://doi.org/10.1128/ ivi.74.24.11825-11831.2000
- 48. Wen F, Blackmon S, Olivier AK, Li L, Guan M, Sun H, Wang PG, Wan XF. 2018. Mutation W222L at the receptor binding site of hemagglutinin could facilitate viral adaption from equine influenza A(H3N8) virus to dogs. J Virol 92:e01115-18. https://doi.org/10.1128/JVI.01115-18
- 49. Yang G, Li S, Blackmon S, Ye J, Bradley KC, Cooley J, Smith D, Hanson L, Cardona C, Steinhauer DA, Webby R, Liao M, Wan X-F. 2013. Mutation tryptophan to leucine at position 222 of haemagglutinin could facilitate H3N2 influenza A virus infection in dogs. J Gen Virol 94:2599–2608. https://doi.org/10.1099/vir.0.054692-0
- Takahashi T, Takano M, Kurebayashi Y, Masuda M, Kawagishi S, Takaguchi M, Yamanaka T, Minami A, Otsubo T, Ikeda K, Suzuki T. 2014. N-glycolylneuraminic acid on human epithelial cells prevents entry of influenza A viruses that possess N-glycolylneuraminic acid binding ability. J Virol 88:8445–8456. https://doi.org/10.1128/JVI.00716-14
- Pettersson SO, Sivertsson R, Sjogren S, Svennerholm L. 1958. The sialic acids of hog pancreas. Biochim Biophys Acta 28:444–445. https://doi. org/10.1016/0006-3002(58)90498-0
- Naiki M. 1971. Chemical and immunochemical properties of two classes of globoside from equine organs. Jpn J Exp Med 41:67–81.
- 53. Song K-H, Kang Y-J, Jin U-H, Park Y-I, Kim S-M, Seong H-H, Hwang S, Yang B-S, Im G-S, Min K-S, Kim J-H, Chang Y-C, Kim N-H, Lee Y-C, Kim C-H. 2010. Cloning and functional characterization of pig CMP-N-acetylneuraminic acid hydroxylase for the synthesis of N-glycolylneuraminic acid as the xenoantigenic determinant in pig-human xenotransplantation. Biochem J 427:179–188. https://doi.org/10.1042/BJ20090835
- Ng PSK, Böhm R, Hartley-Tassell LE, Steen JA, Wang H, Lukowski SW, Hawthorne PL, Trezise AEO, Coloe PJ, Grimmond SM, Haselhorst T, von Itzstein M, Paton AW, Paton JC, Jennings MP. 2014. Ferrets exclusively synthesize Neu5Ac and express naturally humanized influenza A virus receptors. Nat Commun 5:5750. https://doi.org/10.1038/ncomms6750
- Peri S, Kulkarni A, Feyertag F, Berninsone PM, Alvarez-Ponce D. 2018.
 Phylogenetic distribution of CMP-Neu5Ac hydroxylase (CMAH), the enzyme synthetizing the proinflammatory human xenoantigen Neu5Gc.
 Genome Biol Evol 10:207–219. https://doi.org/10.1093/gbe/evx251
- Schauer R, Srinivasan GV, Coddeville B, Zanetta J-P, Guérardel Y. 2009.
 Low incidence of N-glycolylneuraminic acid in birds and reptiles and its absence in the platypus. Carbohydr Res 344:1494–1500. https://doi.org/ 10.1016/j.carres.2009.05.020
- Hoffmann E, Stech J, Guan Y, Webster RG, Perez DR. 2001. Universal primer set for the full-length amplification of all influenza A viruses. Arch Virol 146:2275–2289. https://doi.org/10.1007/s007050170002
- Hoffmann E, Neumann G, Kawaoka Y, Hobom G, Webster RG. 2000. A DNA transfection system for generation of influenza A virus from eight plasmids. Proc Natl Acad Sci U S A 97:6108–6113. https://doi.org/10. 1073/pnas.100133697
- Li L, Liu Y, Ma C, Qu J, Calderon AD, Wu B, Wei N, Wang X, Guo Y, Xiao Z, Song J, Sugiarto G, Li Y, Yu H, Chen X, Wang PG. 2015. Efficient chemoenzymatic synthesis of an N-glycan isomer library. Chem Sci 6:5652–5661. https://doi.org/10.1039/C5SC02025E
- Wen F, Li L, Zhao N, Chiang MJ, Xie H, Cooley J, Webby R, Wang PG, Wan XF. 2018. A Y161F hemagglutinin substitution increases thermostability

- and improves yields of 2009 H1N1 influenza A virus in cells. J Virol 92:e01621-17. https://doi.org/10.1128/JVI.01621-17
- Guan M, Hall JS, Zhang X, Dusek RJ, Olivier AK, Liu L, Li L, Krauss S, Danner A, Li T, Rutvisuttinunt W, Lin X, Hallgrimsson GT, Ragnarsdottir SB, Vignisson SR, TeSlaa J, Nashold SW, Jarman R, Wan X-F. 2019. Aerosol transmission of gull-origin iceland subtype H10N7 influenza A virus in ferrets. J Virol 93:e00282-19. https://doi.org/10.1128/JVI.00282-19
- Xiong X, Tuzikov A, Coombs PJ, Martin SR, Walker PA, Gamblin SJ, Bovin N, Skehel JJ. 2013. Recognition of sulphated and fucosylated receptor sialosides by A/Vietnam/1194/2004 (H5N1) influenza virus. Virus Res 178:12–14. https://doi.org/10.1016/j.virusres.2013.08.007
- Emsley P, Cowtan K. 2004. Coot: model-building tools for molecular graphics. Acta Crystallogr D Biol Crystallogr 60:2126–2132. https://doi. org/10.1107/S0907444904019158
- Liebschner D, Afonine PV, Baker ML, Bunkóczi G, Chen VB, Croll TI, Hintze B, Hung LW, Jain S, McCoy AJ, Moriarty NW, Oeffner RD, Poon BK, Prisant MG, Read RJ, Richardson JS, Richardson DC, Sammito MD, Sobolev OV, Stockwell DH, Terwilliger TC, Urzhumtsev AG, Videau LL, Williams CJ, Adams PD. 2019. Macromolecular structure determination using X-rays, neutrons and electrons: recent developments in Phenix. Acta Cryst D Struct Biol 75:861–877. https://doi.org/10.1107/S2059798319011471

- Reed LJ, Muench H. 1938. A simple method of estimating fifty per cent endpoints. Am J Epidemiol 27:493–497. https://doi.org/10.1093/ oxfordjournals.aje.a118408
- 66. Sun H, Yang J, Zhang T, Long LP, Jia K, Yang G, Webby RJ, Wan XF. 2013.
 Using sequence data to infer the antigenicity of influenza virus. mBio 4:e00230-13. https://doi.org/10.1128/mBio.00230-13
- Edgar RC. 2004. MUSCLE: a multiple sequence alignment method with reduced time and space complexity. BMC Bioinformatics 5:113. https:// doi.org/10.1186/1471-2105-5-113
- Price MN, Dehal PS, Arkin AP. 2009. FastTree: computing large minimum evolution trees with profiles instead of a distance matrix. Mol Biol Evol 26:1641–1650. https://doi.org/10.1093/molbev/msp077
- Martin PT, Golden B, Okerblom J, Camboni M, Chandrasekharan K, Xu R, Varki A, Flanigan KM, Kornegay JN. 2014. A comparative study of Nglycolylneuraminic acid (Neu5Gc) and cytotoxic T cell (CT) carbohydrate expression in normal and dystrophin-deficient dog and human skeletal muscle. PLoS One 9:e88226. https://doi.org/10.1371/journal.pone. 0088226